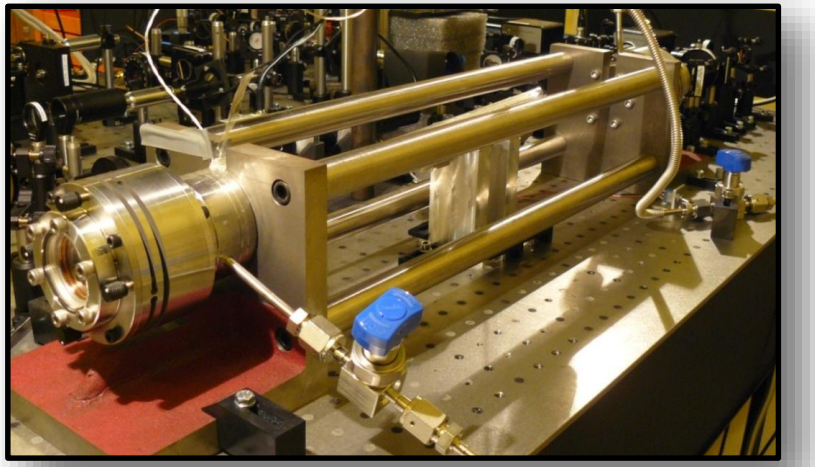

Optical spectroscopy techniques

Daniel Lisak

Nicolaus Copernicus University in Toruń

Outline

- Principles
  - Spectrometers, interferometers
  - Optical absorption spectroscopy
- Fourier-transform spectroscopy
- Laser absorption spectroscopy
  - Frequency modulation
- Photoacoustic spectroscopy
- Laser induced fluorescence
- Doppler-free spectroscopy in molecular beams
- Nonlinear absorption -saturation spectroscopy
- Doppler-free two-photon spectroscopy
- Raman spectroscopy
- Cavity-enhanced laser absorption spectroscopy
  - Cavity ring-down spectroscopy
  - Cavity mode-width and cavity mode-dispersion spectroscopy

Principles

Lambert-Beer law of linear absorption $\mathrm{d}I = -\alpha I \,\mathrm{d}x$

$$I_t(\nu) = I_0 \, \mathrm{e}^{-\alpha(\nu)x}$$

N_k , N_i – population densities of levels *k* and *i*

$$\alpha(\nu_{ki}) = [N_k - (g_k/g_i)N_i]\sigma(\nu_{ki})$$

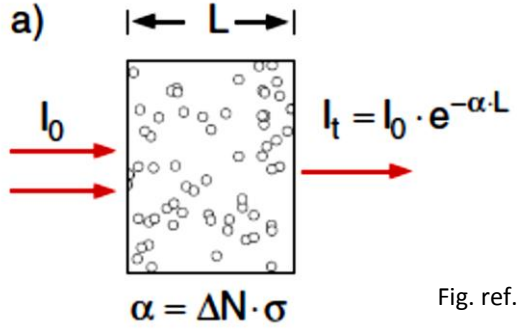

Fig. ref. [1]

g_k , g_i – statistical weights – number of possible orientation of the total angular momentum *J* of the levels
The absorption cross-section σ_{ki} is related to the Einstein coeff. B_{ki}:

$$B_{ki} = \frac{c}{h\nu_{ki}} \int_{\nu=0}^{\infty} \sigma(\nu)\, \mathrm{d}\nu$$

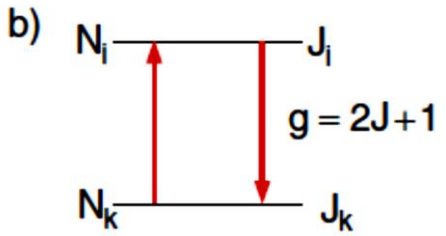

$$\Delta N = (N_k - \frac{g_k}{g_i} N_i)$$

Fig. ref. [1]

Approximation for small absorption:

$$I_t(\nu) \approx I_0(1 - \alpha(\nu)x)$$

$$\frac{\Delta I}{I_0} = \frac{I_0 - I_t}{I_0} \approx \alpha(\nu)L = [N_k - (g_k/g_i)N_i]\,\sigma(\nu_{ik})L = \Delta N_{ik} \cdot \sigma(\nu_{ik})L$$

Minimum detectable intensity change ΔI depends on the intensity noise level ΔI_{noise}
For detector signal $S \sim \Delta I$ and detector signal noise $\delta S \sim \Delta I_{\text{noise}}$
Sensitivity is a signal-to-noise ratio: $S/\delta S$
From condition $S \geq \delta S \Rightarrow \Delta I \geq \Delta I_{\text{noise}}$ the minimum detectable number density of absorbing molecules:

$$\Delta N \geq \frac{1}{\sigma(\nu_{ki})L(S/\delta S)}$$

ΔN depends on:
path length,
signal-to-noise ratio,
absorption cross-section

[1] W. Demtroder, Atoms, molecules and photons

Principles

Spectral resolving power *R*

$$R = \lambda / \Delta\lambda_{\min}$$

Rayleigh definition – lines are resolved if there is a dip of less than 0.8 of maximum between them

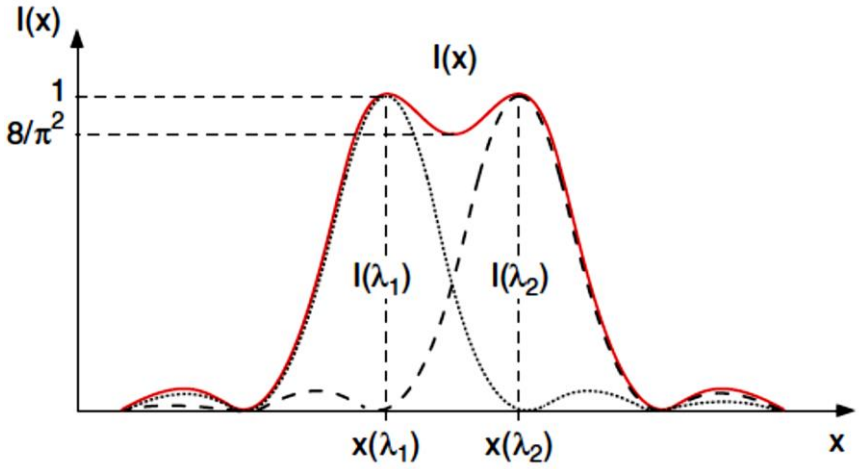

Fig. ref. [1]

$\Delta\lambda_{\min}$ depends on:

- spectral line shapes
  (natural line width, collisional and Doppler broadening)
- spectroscopic instrument – instrumental function
  (spectrometer, interferometer)

Principles

Spectroscopic instruments

Spectrometers – allow the spatial dispersion of different wavelengths

- refracting prism
- diffraction grating

Angular dispersion $\frac{d\Theta}{d\lambda}$ and linear dispersion $\frac{dx}{d\lambda}$

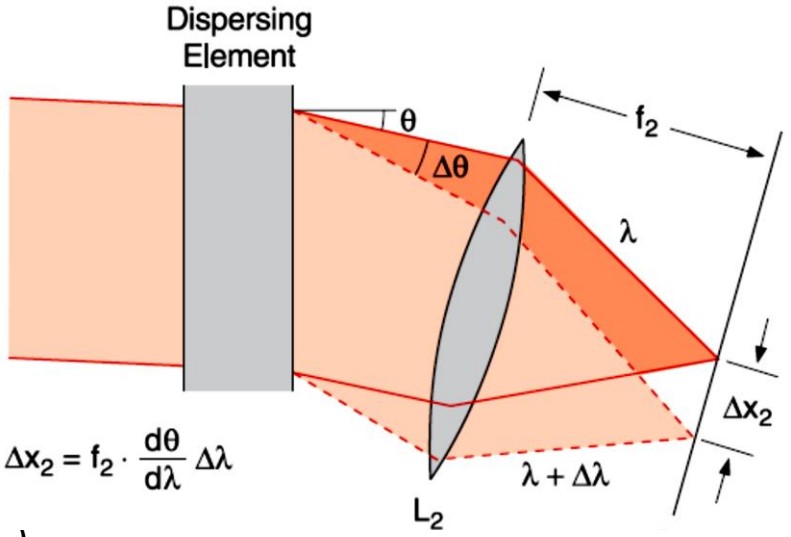

Resolution limited by diffraction on the aperture *a* (of grating, prism, lens…)

$$\delta\lambda \geq 2(\lambda/a)/(d\Theta/d\lambda) \qquad (*)$$

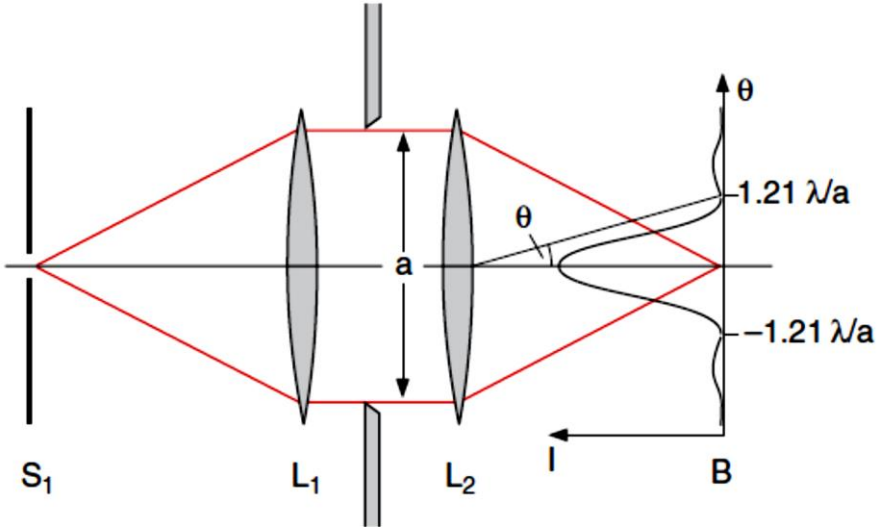

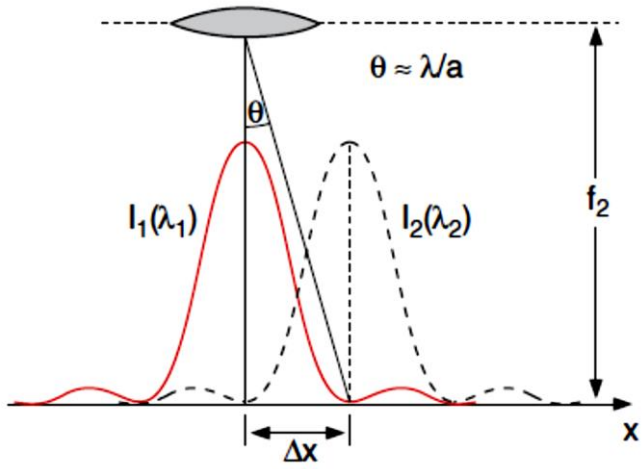

Figs. ref. [1]

Principles

Prism spectrometer

From geometrical optics

$$\frac{\sin(\Theta+\varepsilon)}{2} = n\sin(\varepsilon/2)$$

The angular dispersion

$$\frac{d\Theta}{d\lambda} = \left(\frac{dn}{d\Theta}\right)^{-1}\cdot\frac{dn}{d\lambda} = \frac{2\sin(\varepsilon/2)}{\sqrt{1-n^2\sin^2(\varepsilon/2)}}\frac{dn}{d\lambda}$$

depends on the apex angle ε. For $\varepsilon = 60°$:

$$\frac{d\theta}{d\lambda} = \frac{dn/d\lambda}{\sqrt{1-(n/2)^2}}$$

For symmetric case $\alpha_1 = \alpha_2$ the diffraction limit for Resolving power (from eq. (*)) is

$$\frac{\lambda}{\Delta\lambda} = g\frac{dn}{d\lambda}$$

depends on the size and prism material

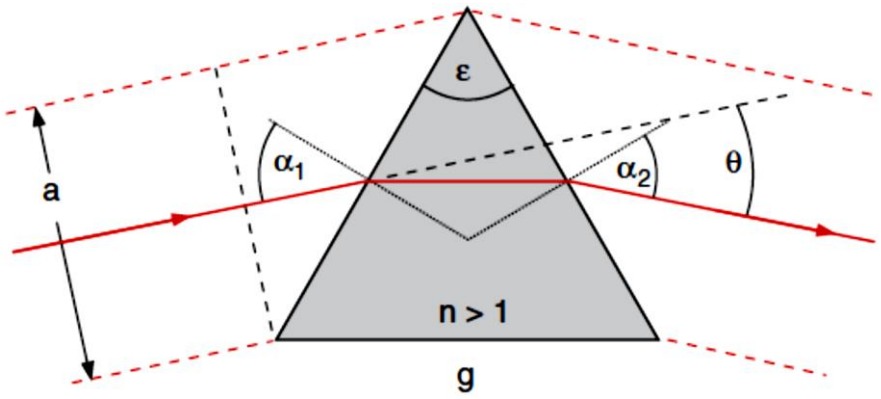

Fig. ref. [1]

Principles

Grating spectrometer

Incident radiation is reflected on each groove into angular cone due to diffraction

constructive interference for phase difference $\Delta\varphi = m \cdot 2\pi$

path difference between two partial waves $\Delta s = d(\sin\alpha - \sin\beta)$

Condition for constructive interference (when $\Delta\varphi = m2\pi \Rightarrow \Delta s = m\lambda$)

$$d(\sin\alpha \pm \sin\beta) = m\lambda \qquad (*)$$

(± for reflection left/right)

Phase difference between neighboring beams

$$\Delta\varphi = \frac{2\pi}{\lambda} \cdot d(\sin\alpha \pm \sin\beta) \qquad (**)$$

Superposition of reflected partial wave amplitudes

$$A_R = \sqrt{R} \sum_{m=0}^{N-1} A_g e^{im\phi}$$

R – reflectivity of grating surface
A_g – amplitude incident on one groove

The **total intensity** is

$$I_R = \varepsilon_0 c A_R A_R^* = I_0 R \frac{\sin^2(N\phi/2)}{\sin^2(\phi/2)} \qquad (***)$$

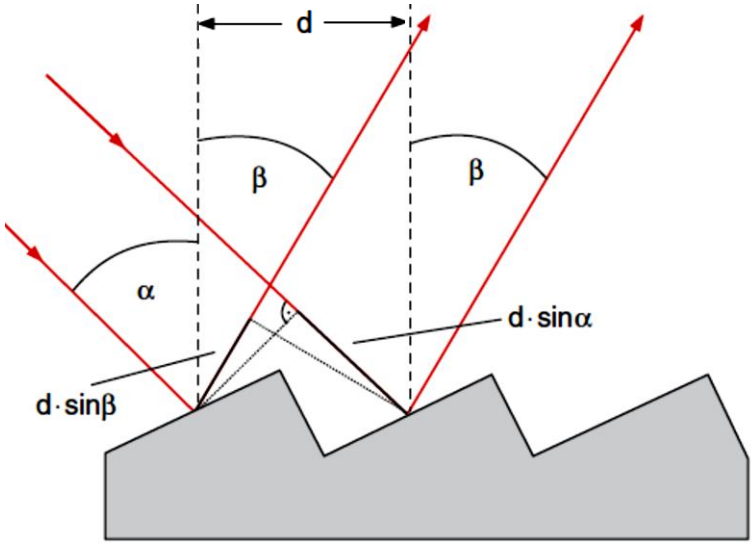

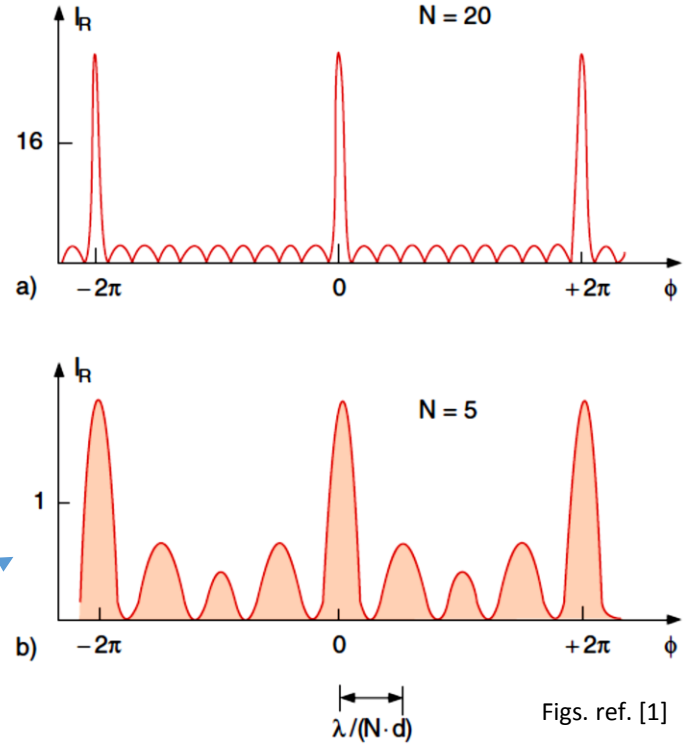

N-2 small side maxima

Figs. ref. [1]

Grating spectrometer

For big *N* radiation with incident angle α and wavelength λ is reflected at narrow angular interval $\Delta\beta$ around the principal maxima β_m

Near β_m: $\beta = \beta_m + \varepsilon \quad (\varepsilon << \beta)$ one can write: $\sin(\beta_m + \varepsilon) \approx \sin\beta_m + \varepsilon \cdot \cos\beta_m$

From (**) and (***):

$$I_R = I_0 R \frac{\sin^2(N\delta/2)}{\sin^2(\delta/2)} \approx R \cdot I_0 N^2 \frac{\sin^2(N\delta/2)}{(N\delta/2)^2}$$

where $\delta = (2\pi d/\lambda)\varepsilon\cos\beta_m \ll 1$

The first minima (left and right) appear for: $N\delta = 2\pi \Rightarrow \varepsilon_{1,2} = \pm\lambda/(Nd\cos\beta_m$

so, the **width** between minima is:

$$\Delta\beta = \frac{\lambda}{Nd\cos\beta_m}$$

Angular dispersion for given α, from derivative of (*):

$$\frac{d\beta}{d\lambda} = \frac{m}{d\cos\beta} = \frac{\sin\alpha \pm \sin\beta}{\lambda\cos\beta}$$

← depends on angles, not number of grooves

Resolving power, from two above eqns:

Condition for resolved peaks: max. I(λ) falls into first min. I(λ+Δλ)

$$\frac{d\beta}{d\lambda}\cdot\Delta\lambda \geq \frac{\lambda}{Nd\cos\beta} \rightarrow \frac{\sin\alpha \pm \sin\beta}{\lambda\cos\beta}\Delta\lambda \geq \frac{\lambda}{Nd\cos\beta}$$

From the above and (*):

$$\frac{\lambda}{\Delta\lambda} \geq N\cdot m \qquad \text{or, since} \quad Nd(\sin\alpha \pm \sin\beta) = \Delta s_m \rightarrow \frac{\lambda}{\Delta\lambda} = \frac{\Delta s_m}{\lambda}$$

Resolving power is a product of number *N* of illuminating grooves and interference order *m*, or it is the maximum paths difference ΔS_m in spectrometer measured in units of wavelength

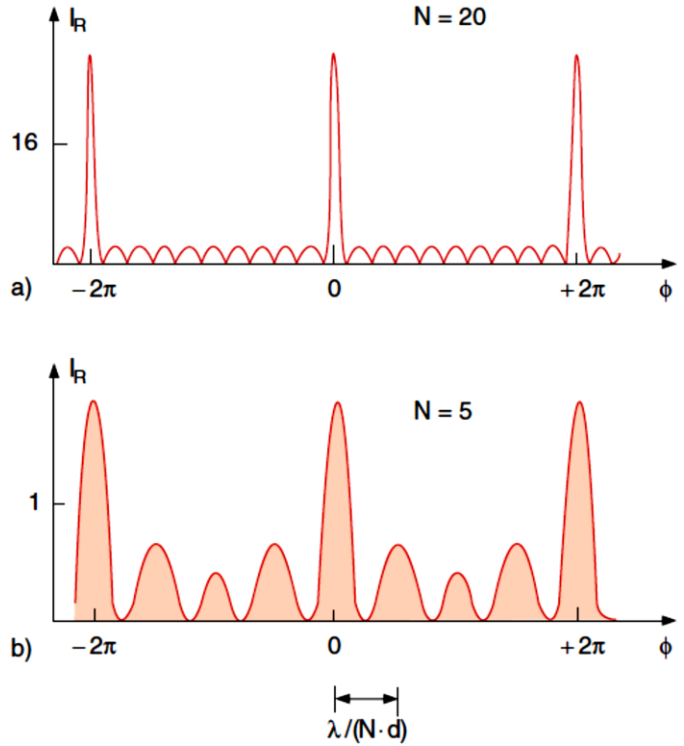

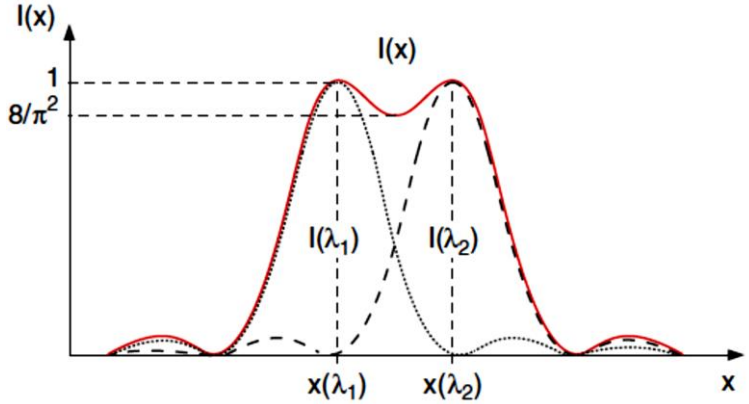

Figs. ref. [1]

Optical absorption spectroscopy

Classical infrared spectrometer

e.g. continuous blackbody thermal radiation: T = 1000 K → I_{max} at 3 µm

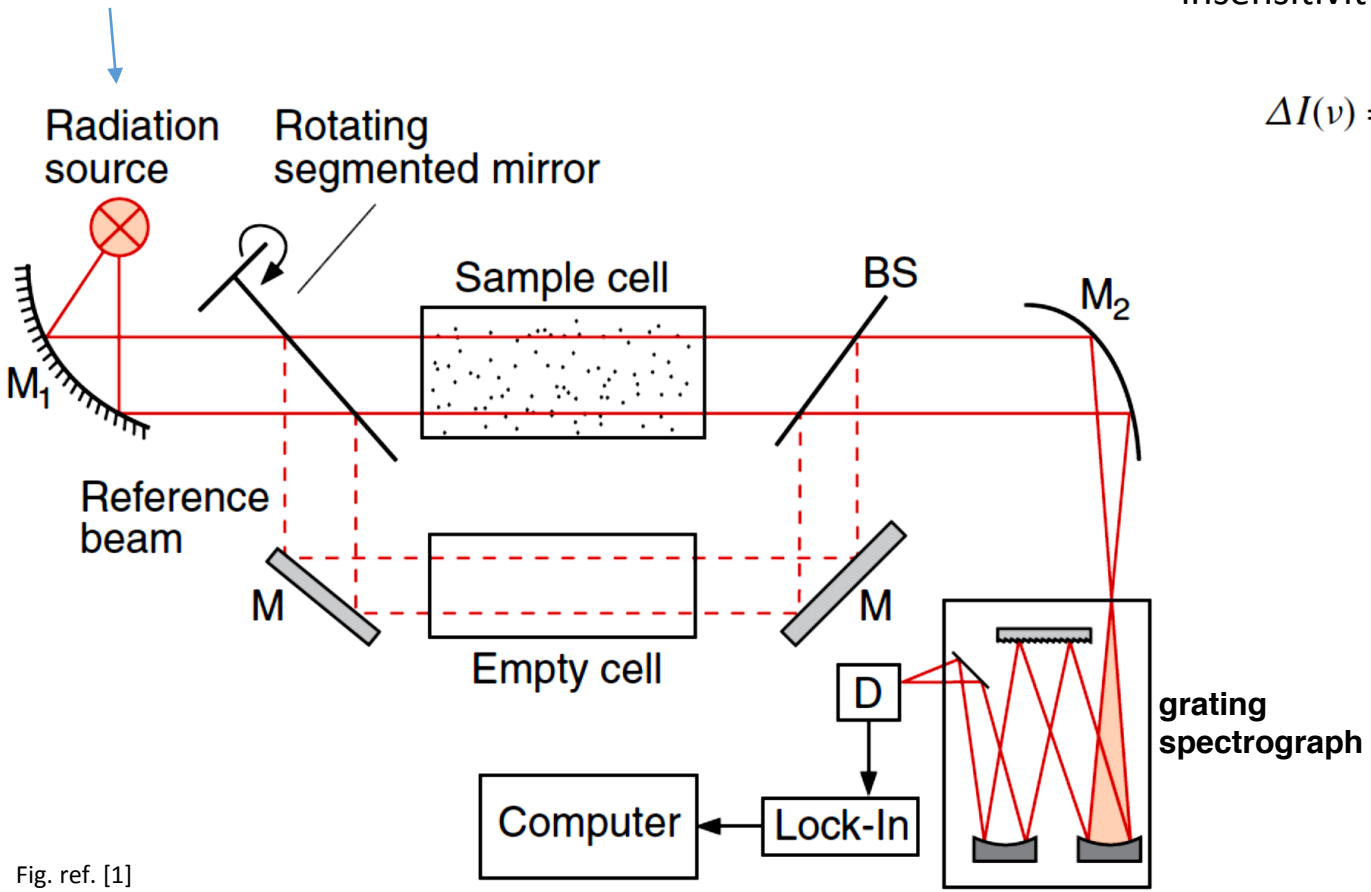

Fig. ref. [1]

Reference intensity I_0 measurement enables insensitivity to source power variations

$$\Delta I(\nu) = I_R - I_t(\nu) = \alpha(\nu) \cdot L \cdot I_0$$

$$\Delta I / I_0 = \alpha(\nu) \cdot L$$

Principles

Fabry-Perot interferometer (multiple-beam interference)

Incident wave $E = A_0 e^{i(\omega t - kr)}$

R – reflectivity of surface

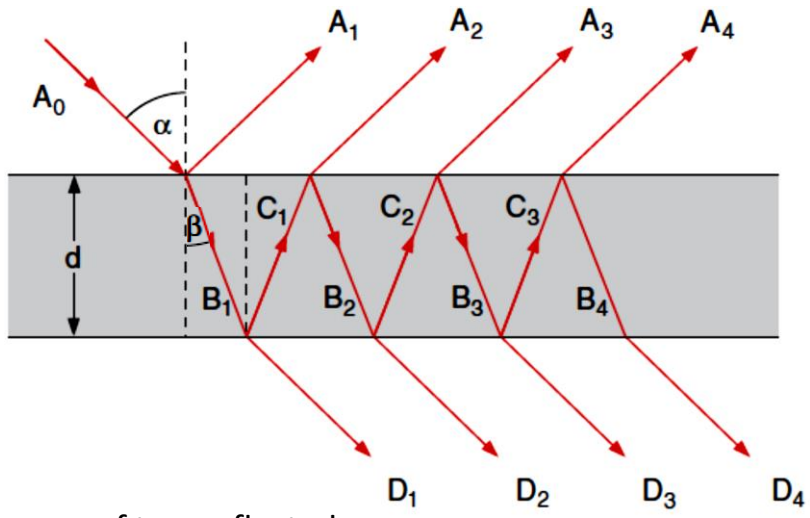

Total amplitude of the reflected wave

$$A = \sum_{m=1}^{p} A_m e^{i(m-1)\Delta\varphi} = \pm A_0 \sqrt{R}\left[1 - (1-R)e^{i\Delta\varphi}\sum_{m=0}^{p-2} R^m e^{im\Delta\varphi}\right]$$

for $p \to \infty$ the sum of geometric series is

$$\sum_{m=1}^{p} A_m e^{im\Delta\varphi} = \frac{1}{1 - R e^{i\Delta\varphi}}$$

$\Delta\varphi = 2\pi\Delta s/\lambda + \delta\varphi$ - phase difference of two reflected waves

$\Delta s = 2d\sqrt{n^2 - \sin^2\alpha}$

reflected amplitude

$$A = \pm\sqrt{R}A_0\frac{1 - e^{i\Delta\varphi}}{1 - R e^{i\Delta\varphi}}$$

And reflected intensity

$$I_R = c\varepsilon_0 |A|^2 = I_0 R\frac{2 - 2\cos\Delta\varphi}{1 + R^2 - 2R\cos\Delta\varphi} = I_0\frac{4R\sin^2(\Delta\varphi/2)}{(1-R)^2 + 4R\sin^2(\Delta\varphi/2)}$$

Similarly, transmitted intensity

$$I_t = I_0\frac{(1-R)^2}{(1-R)^2 + 4R\sin^2(\Delta/2)}$$

Airy formulas

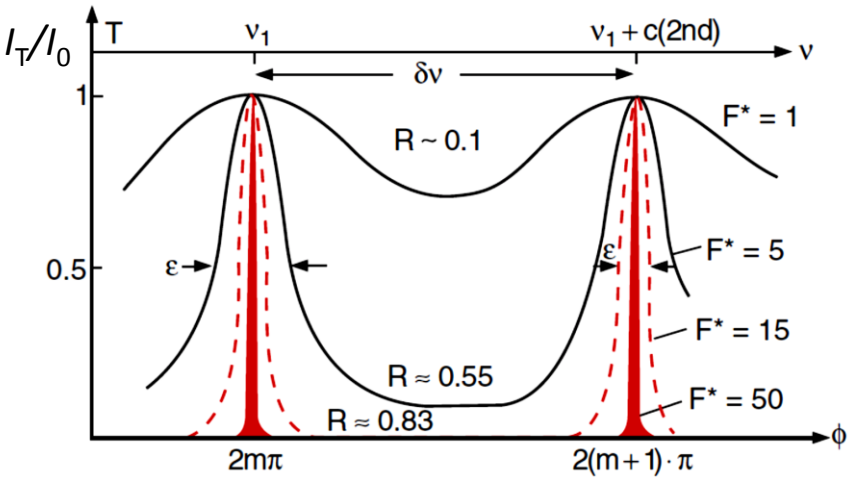

Figs. ref. [1]

Principles

Fabry-Perot interferometer (multiple-beam interference)

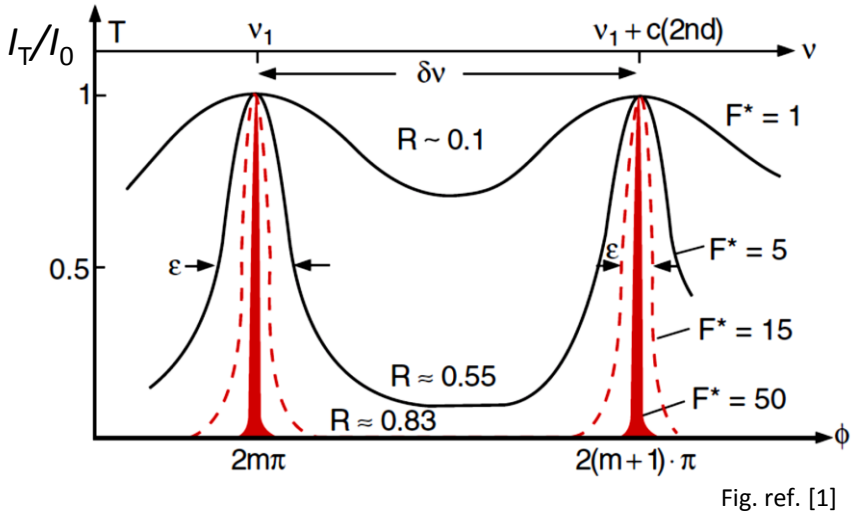

Fig. ref. [1]

Separation of two maxima – free spectral range

$$\delta\nu = \frac{c}{\Delta s} = \frac{c}{2d\sqrt{n^2 - \sin^2\alpha}}$$

$$\delta\nu(\alpha = 0) = \frac{c}{2nd}$$

Full half-width of transmission peak (in phase units)

$$\epsilon = 4\arcsin\left(\frac{1-R}{2\sqrt{R}}\right) \approx \frac{2(1-R)}{\sqrt{R}} \quad \leftarrow \quad \text{for } R \approx 1$$

In frequency units:

$$\Delta\nu = \frac{\epsilon}{2\pi}\delta\nu \simeq \frac{c}{2nd}\frac{1-R}{\pi\sqrt{R}}$$

Finesse *F**

$$F_R^* = \frac{\delta\nu}{\Delta\nu} = \frac{\pi\sqrt{R}}{1-R}$$

is a measure of effective number of interfering partial waves

Resolving power of FPI: $\nu/\Delta\nu = (\nu/\delta\nu)F^*$

Or using optical path difference Δs between consecutive partial waves:

$$\frac{\nu}{\Delta\nu} = \frac{\lambda}{\Delta\lambda} = F^*\frac{\Delta s}{\lambda}$$

product of finesse (number of partial waves) and optical path difference (in units of wavelength) – similar to diffraction grating

Principles

Fabry-Perot interferometer

Resolving power of FPI can be much higher than that of diffraction grating

Scanning Fabry-Perot + diffraction grating spectrometer

high resolution low resolution - separation of interference orders

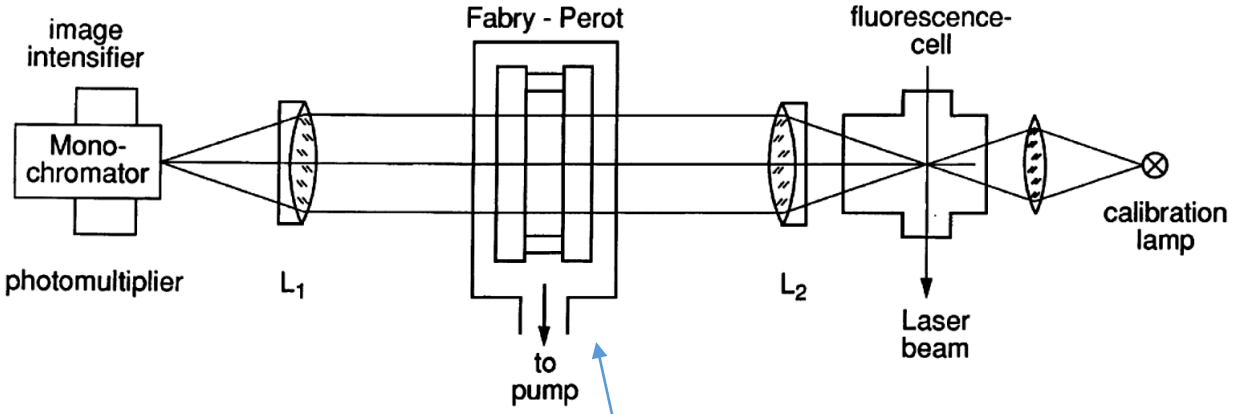

Free spectral range

$$\delta\nu(\alpha = 0) = \frac{c}{2nd}$$

Change of: refractive index n (gas pressure)
spacer length d (piezo voltage)
shifts FPI transmission peaks

Convolution of the Airy formula for FPI transmission and molecular line shape

Example scan of Doppler-broadened Na_2 fluorescence line and narrow single-mode Ar laser line

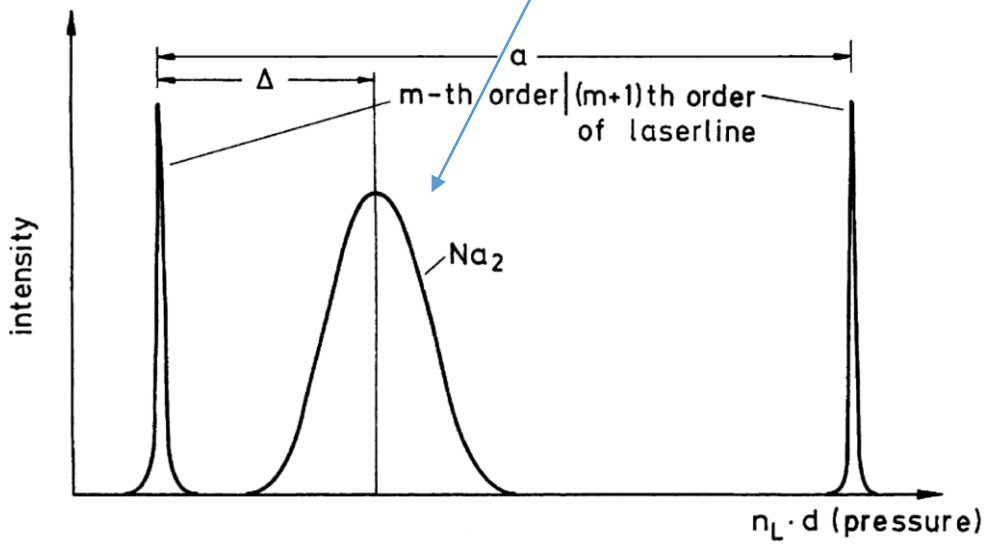

[2] W. Demtroder, Laser spectroscopy

Figs. ref. [2]

Michelson interferometer & Fourier Transform Spectroscopy

Incident radiation: $E(\omega) = A_0 \cos \omega_0 t$

$$I(\omega) = c\varepsilon_0 E^2 = c\varepsilon_0 A_0^2 \cos^2 \omega_0 t = I_0 \cos^2 \omega_0 t$$

Amplitudes of two interfering partial waves: $A_i = \sqrt{RT}\, A_0$
Intensity at plane B depends on path difference $\Delta s = s_1 - s_2$

$$\begin{aligned} I_t &= c\varepsilon_0 RT A_0^2 [\cos(\omega_0 t + k s_1) + \cos(\omega_o t + k s_2)]^2 \\ &= RTI_0 \big[\cos^2(\omega_0 t + k s_1) + \cos^2(\omega_0 t + k s_2) \\ &\quad + \cos(2\omega_0 t + k(s_1 + s_2)) + \cos(k(s_1 - s_2)) \big] \end{aligned}$$

Detector averages high optical frequencies:

$\langle \cos \omega_0 t \rangle = 0 \qquad \langle \cos^2 \omega_0 t \rangle = \frac{1}{2}$

So its signal is:

$$S(t) \propto \langle I(t) \rangle = RTI_0 \left[1 + \cos\left(\omega_0 \frac{v}{c} t \right) \right]$$

where
$s_2 = s_1 + vt$
$k = \omega_0 / c$

Optical frequency is transformed into much lower frequency

$\omega_0 \longrightarrow \Omega = \omega_0 v / c$

Mathematically spectrum $I(\omega)$ is a **Fourier transform** of detector signal $S(t)$

$$I(\omega) = \lim_{\tau \to \infty} \int_{t=0}^{\tau} S(t) \cos\left(\omega \frac{v}{c} t \right) \, \mathrm{d}t$$

Michelson interferometer with continuously and uniformly changed path length of one arm

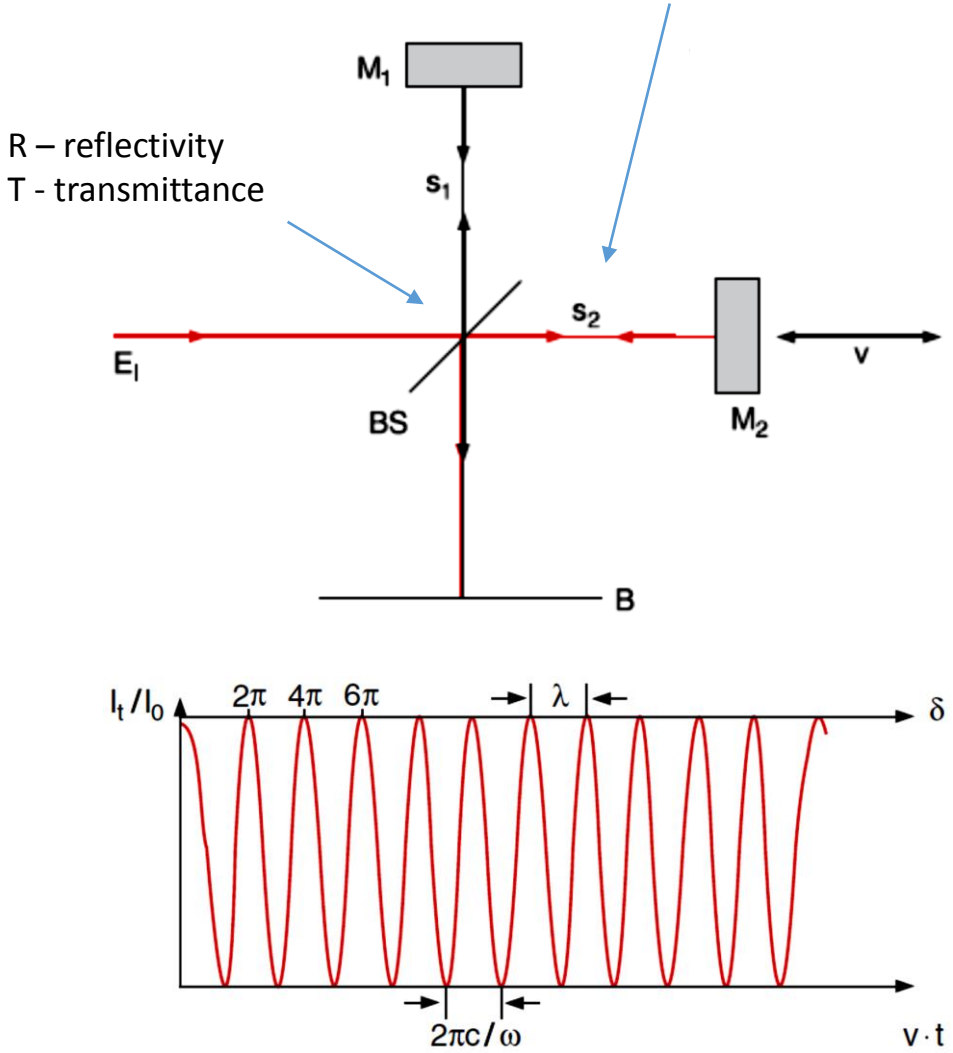

Figs. ref. [1]

Fourier Transform Spectroscopy

Radiation containing two frequencies: ω_1 and ω_2
Superposition of interferograms for two monochromatic waves
Detector signal is

$$S(t) \propto RT\bar{I}_0\left[1+2\cos\left(\frac{\omega_1-\omega_2}{2}\frac{v}{c}t\right)\cos\left(\frac{\omega_1+\omega_2}{2}\frac{v}{c}t\right)\right]$$

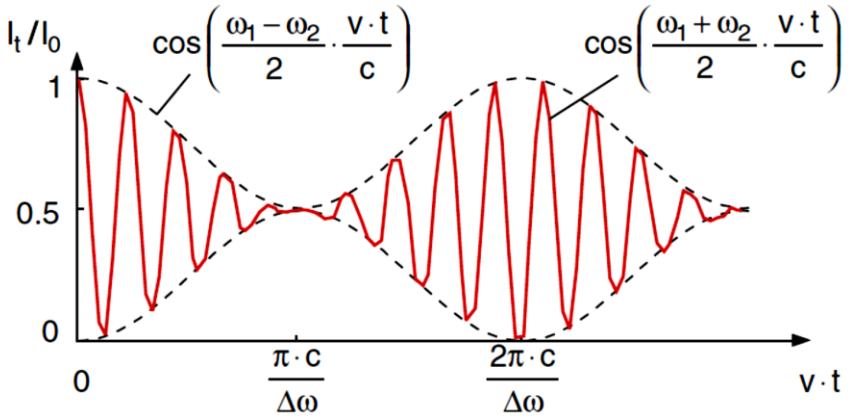

Figs. ref. [1]

To find frequencies ω_1, ω_2 from measured signal $S(t)$ at least one beat period $T = (\frac{2\pi c}{v})/(\omega_1 - \omega_2)$ must be measured.

Relation between minimum frequency difference $\delta\omega = (\omega_1 - \omega_2)$ and minimum measurement time Δt or path difference $\Delta s = v\Delta t$

$$\frac{v}{t}\delta\omega \geq \frac{2\pi}{\Delta t} \Rightarrow \delta\omega \geq \frac{2\pi c}{\Delta s}$$

Max. path difference Δs between interfering partial waves (in wavelength units) gives the **resolving power** $\omega/\delta\omega$ of the interferometer

$$\frac{\omega}{\delta\omega} = \frac{2\pi\nu}{\delta\omega} = \frac{2\pi c\Delta s}{\lambda\cdot 2\pi c} = \frac{\Delta s}{\lambda}$$

General case: radiation with many frequencies:

$$S(t) = a\int_0^\infty \bar{I}_0(\omega)\left[1+\cos\left(\omega\frac{v}{c}t\right)\right]\mathrm{d}\omega$$

Intensity spectrum of the radiation source is a Fourier transform of $S(t)$. $\tau = \Delta t$ is measurement time

$$\bar{I}(\omega) = \lim_{\tau\to\infty}\frac{b}{\tau}\int_0^\tau S(t)\cos\left(\omega\frac{v}{c}t\right)\mathrm{d}t$$

Fourier Transform Spectroscopy

Intensity spectrum of the radiation source is a Fourier transform of $S(t)$. $\tau = \Delta t$ is measurement time

$$\overline{I}(\omega) = \lim_{\tau\to\infty} \frac{b}{\tau} \int_0^{\tau} S(t) \cos\left(\omega \frac{v}{c} t\right) \mathrm{d}t$$

Mathematically FT has integration limits 0 to ∞, therefore a gate function is used for finite experimental data

$$\overline{I}(\omega) = \int_0^{\infty} S(t)G(t) \cos\left(\omega \frac{v}{c} t\right) \mathrm{d}t$$

where

$$G(t) = \begin{cases} 1 \ \text{ for } 0 \le t \le t_{\max} \\ 0 \ \text{ for } t > t_{\max} \end{cases} \qquad t_{\max} = \Delta s_{\max}/v$$

FT of rectangular function leads to $(\sin x\,/x)^2$ diffraction-like structure (like transmission through rectangular slit)

Gaussian function can be used instead of rectangle to eliminate diffraction effects. Function can be optimized to minimize influence on spectrum.

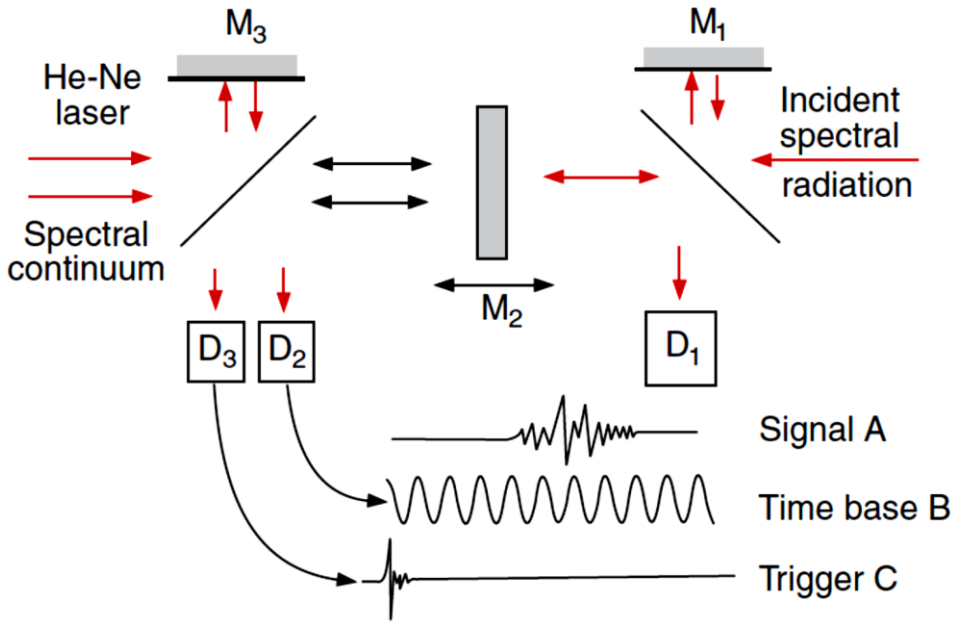

Figs. ref. [1]

Scheme of FT spectrometer with reference He-Ne laser for time base measurement and spectral continuum for $t = 0$ (equal arms, $\Delta s = 0$) measurement

Fourier Transform Spectroscopy

Advantages of FTS:

(comparing to traditional spectroscopy)

- high resolution $\frac{\omega}{\delta\omega} = \frac{\Delta s}{\lambda}$
- high signal-to-noise ratio

(all frequencies are measured simultaneously)

(comparing to laser spectroscopy)

- faster broadband spectrum

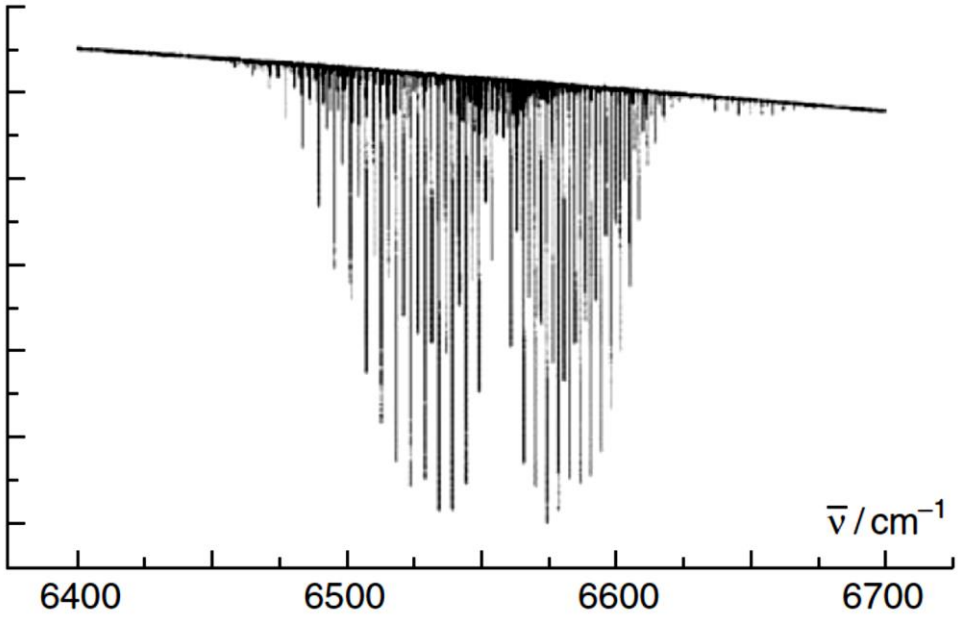

Figs. ref. [2]

Weak overtone band of C_2H_2 with rotational structure resolved by FTS

Laser Absorption Spectroscopy

- No need of dispersive wavelength separation
- Single-mode tunable laser – monochromatic source
- Resolution limited only by molecular line width
- Well collimated laser beam enables long path absorption cell configurations (multi-pass or resonant cells) – high sensitivity
- No instrumental function – precise line profile measurement

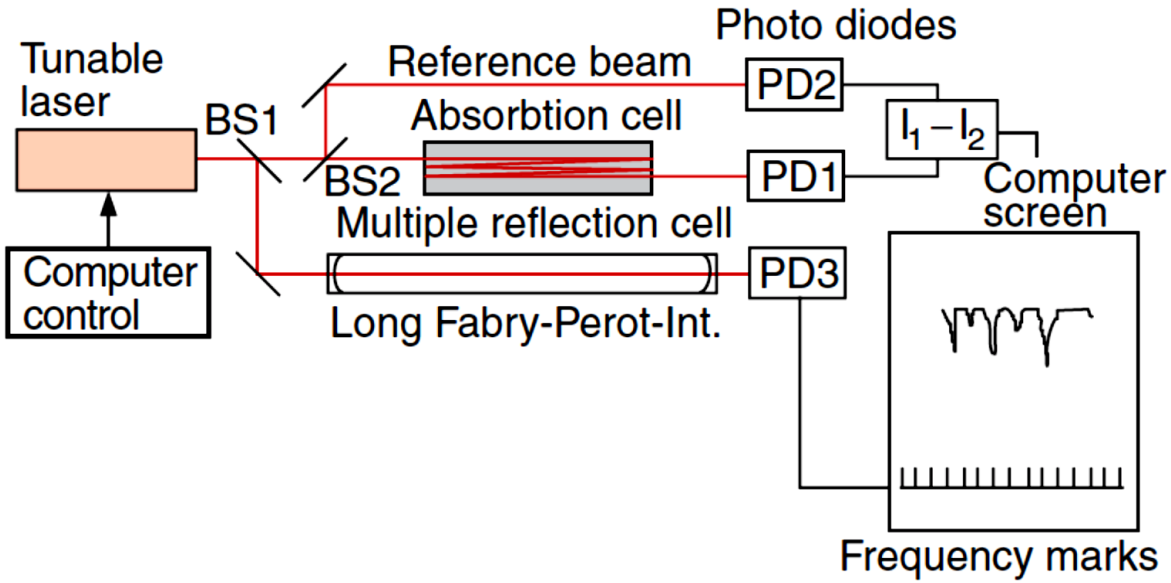

Laser absorption spectroscopy setup

Figs. ref. [1]

Laser Absorption Spectroscopy – frequency modulation scheme

Elimination of laser power variation influence

Modulation with frequency Ω changes the laser frequency ω_L by $\Delta\omega_L$.
Transmission difference ΔP_T is detected

$$\Delta P_{\mathrm{T}} = P_{\mathrm{T}}(\omega_{\mathrm{L}} - \Delta\omega_{\mathrm{L}}/2) - P_{\mathrm{T}}(\omega_{\mathrm{L}} + \Delta\omega_{\mathrm{L}}/2)$$

with phase-sensitive detector at freq. Ω.
Taylor expansion

$$\Delta P_{\mathrm{T}}(\omega) = \frac{\mathrm{d}P_{\mathrm{T}}}{\mathrm{d}\omega}\Delta\omega_{\mathrm{L}} + \frac{1}{2!}\frac{\mathrm{d}^2 P_{\mathrm{T}}}{\mathrm{d}\omega^2}\Delta\omega_{\mathrm{L}}^2 + \ \ldots$$

The first term (dominant for small $\Delta\omega_L$) is proportional to derivative of absorption coefficient

$$\frac{\mathrm{d}\alpha(\omega)}{\mathrm{d}\omega} = -\frac{1}{P_{\mathrm{R}} L}\frac{\mathrm{d}P_{\mathrm{T}}}{\mathrm{d}\omega}$$

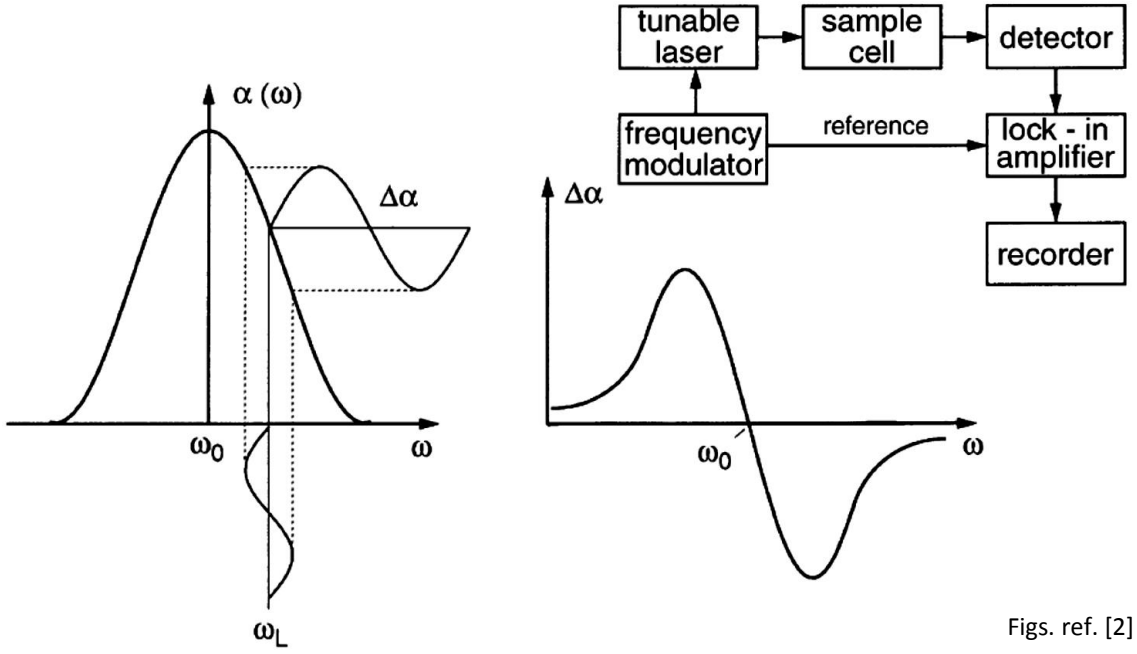

Figs. ref. [2]

Laser Absorption Spectroscopy – frequency modulation scheme

Higher derivatives of α can be also achieved

For modulated laser frequency $\omega_L(t) = \omega_0 + a \sin \Omega t$
from Taylor expansion

$$P_T(\omega_L) = P_T(\omega_0) + \sum_n \frac{a^n}{n!} \sin^n \Omega t \left(\frac{d^n P_T}{d\omega^n} \right)_{\omega_0}$$

for low absorption ($\alpha L \ll 1$) we obtain from $P_T(\omega) \simeq P_0[1 - \alpha(\omega)x]$

$$\left(\frac{d^n P_T}{d\omega^n} \right)_{\omega_0} = -P_0 x \left(\frac{d^n \alpha(\omega)}{d\omega^n} \right)_{\omega_0}$$

From trigonometric transformation – one obtains for small modulation $(a/\omega_0 \ll 1)$ that signal after lock-in amplifier, tuned to frequencies $n\Omega$ (n=1,2,3) is proportional to n-th derivative of α

$$S(\Omega) = -aL \frac{d\alpha}{d\omega} \sin(\Omega t) ,$$

$$S(2\Omega) = +\frac{a^2 L}{4} \frac{d^2\alpha}{d\omega^2} \cos(2\Omega t)$$

$$S(3\Omega) = +\frac{a^3 L}{24} \frac{d^3\alpha}{d\omega^3} \sin(3\Omega t)$$

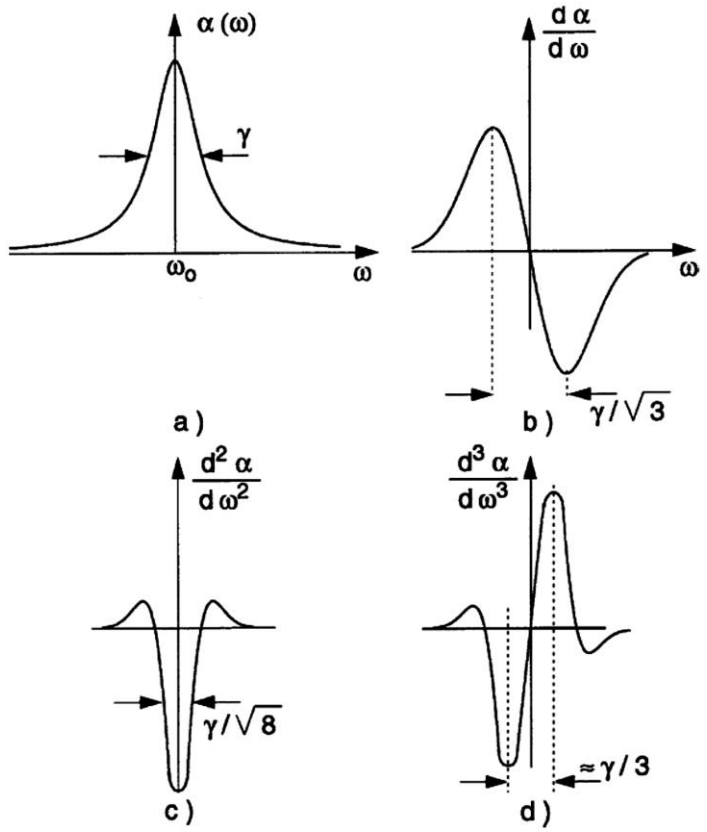

Figs. ref. [2]

Laser Absorption Spectroscopy – frequency modulation scheme

Phase φ modulation scheme with electro-optic modulator (EOM)
$\omega = \mathrm{d}\varphi/\mathrm{d}t$ sidebands at $\omega \pm \Omega$

sidebands with opposite phase

cancel each other

don't cancel

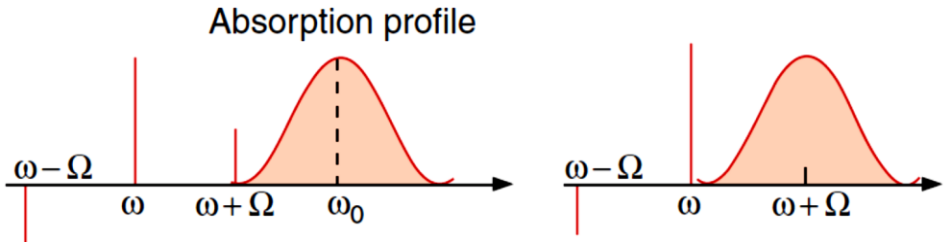

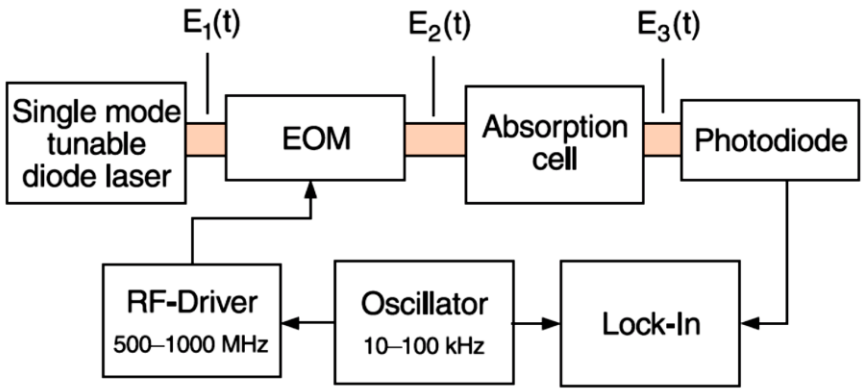

Phase-modulation spectroscopy setup

no modulation

phase modulation

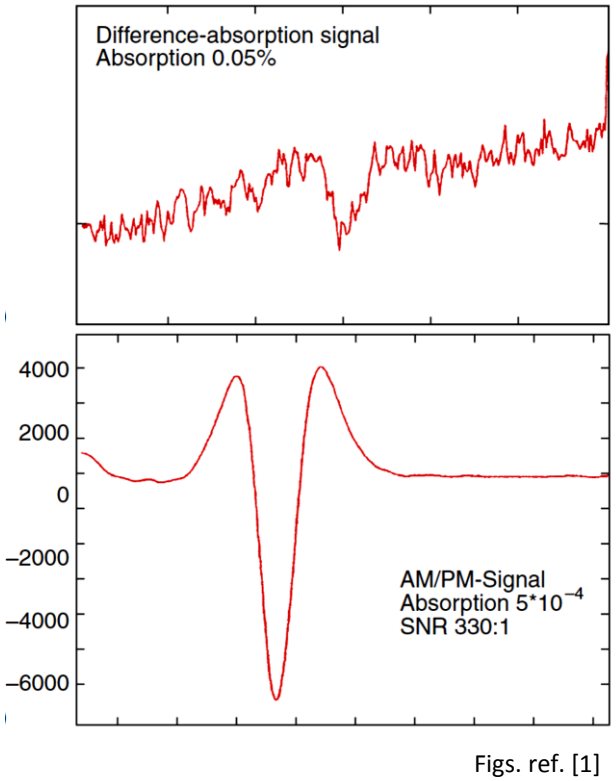

Figs. ref. [1]

Improvement in SNR of H_2O absorption line due to phase-modulation spectroscopy

Photoacoustic spectroscopy

N absorbing molecules in a cell with volume *V*

Excited $E_i = E_k + h\nu$ molecules can transfer excitation energy into other molecule kinetic energy by collisions $E_{\text{kin}} = \frac{3}{2}NkT$
and gas temperature increases

$$\Delta T = \frac{N_1 h\nu}{\frac{3}{2}Nk}$$

N_1 – no. of excited molecules

This leads to pressure change

$$\Delta p = nk\Delta T$$

$n = N/V$

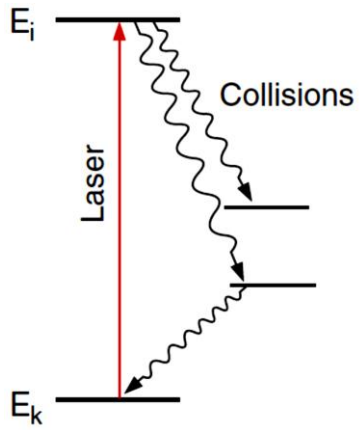

laser beam amplitude is modulated with frequency
$f <$ inverse of energy transfer time $(1/\tau_{\text{coll}} + 1/\tau_{\text{rad}})$
Then presure is modulated with frequency f.
This accoustic wave is registered
by microphone

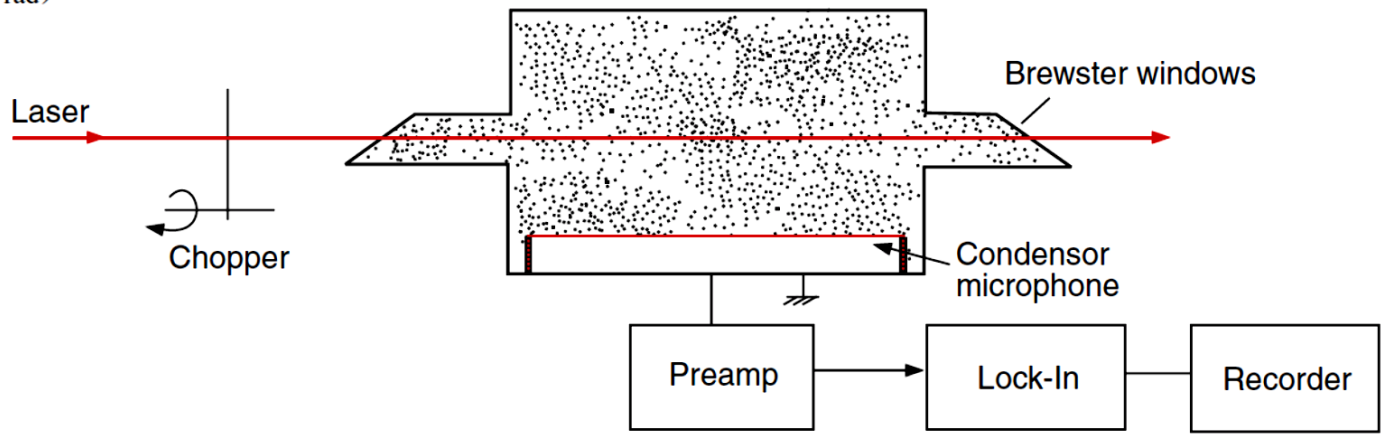

Absorbed photon energy is converted into acoustic energy

Frequency f can be tuned to accoustic eigenresonance of the cell → standing wave

Amplitude increased by *Q* factor of the cell

Figs. ref. [1]

Photoacoustic spectroscopy

Sensitivity of PAS can be further increased by using multipass cell or a resonant optical cavity

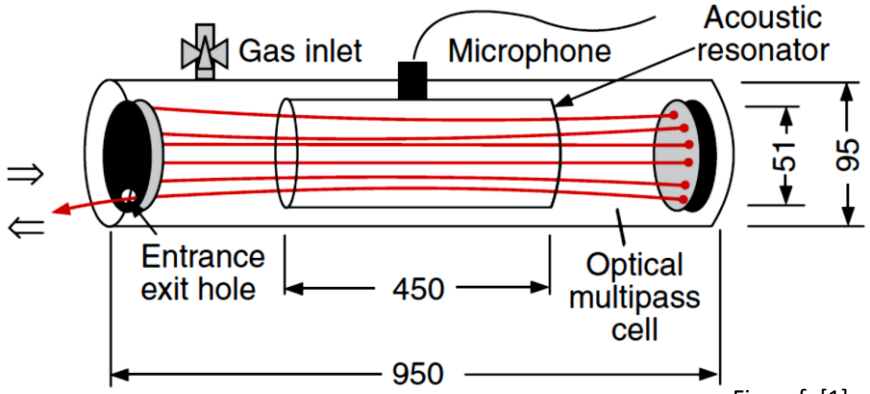

Fig. ref. [1]

noise equivalent absorption ~ 10^{-10} cm^{-1} $Hz^{-1/2}$ can be achieved

high sensitivity requires relatively high pressure (accoustic wave), like e.g. detection of trace gases in atmosphere

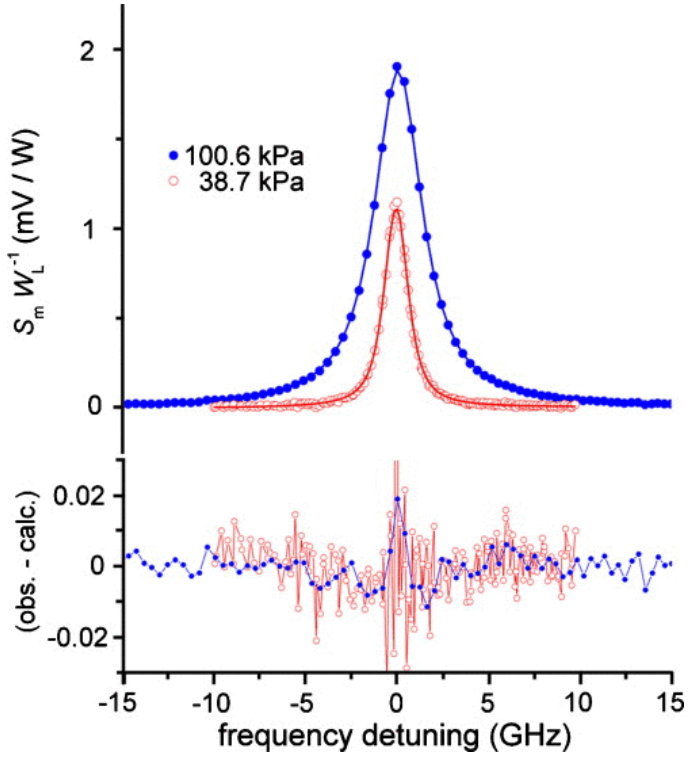

PAS spectra of O_2, A-band line

Gills et al., Rev. Sci. Instrum. 81, 064902 (2010)

Laser induced fluorescence

Selective excitation of one or a few levels in the upper state of atoms or molecules

Spontaneous emission in all directions

If one upper level is excited – spectrum gives energy differences between lower states

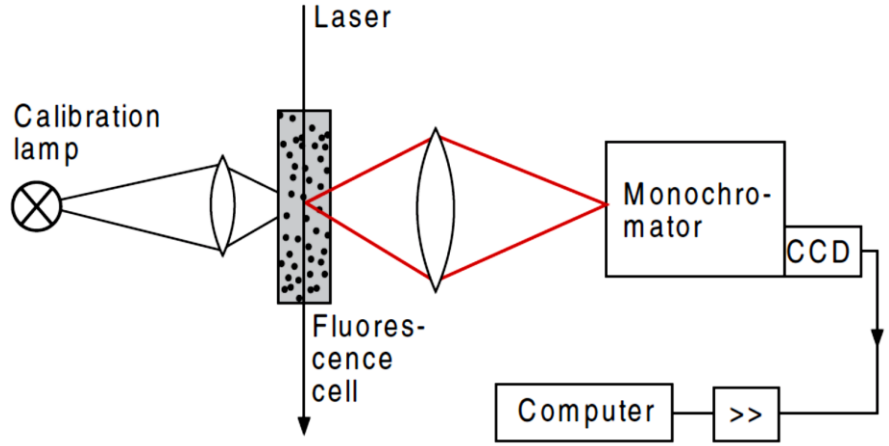

Laser induced fluorescence experimental setup

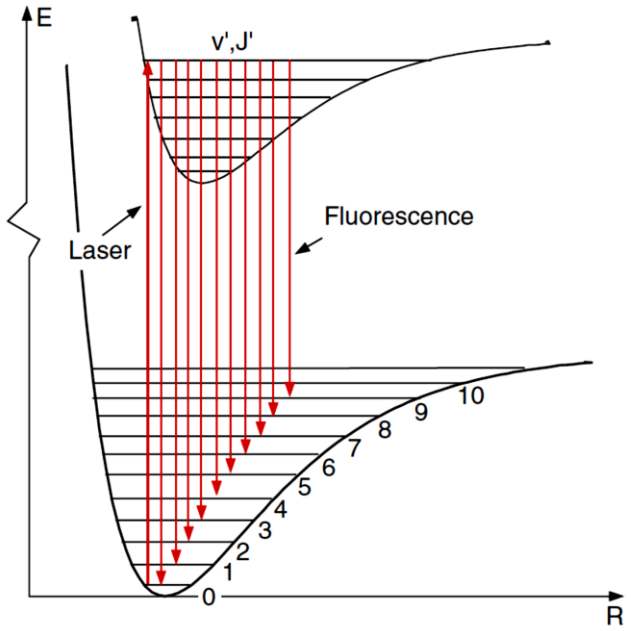

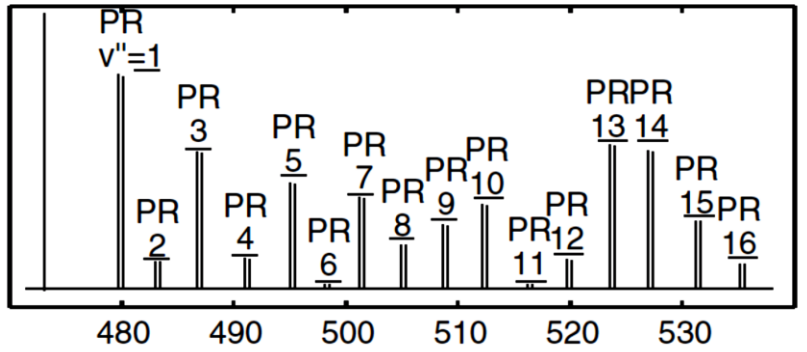

Figs. ref. [1]

Energy levels and LIF spectrum of Na_2 molecule

Laser induced fluorescence

Total fluorescence signal is proportional to the absorption spectrum:

Excitation spectroscopy - very sensitive technique

Signal *S* (rate of photoelectrons $\dot{n}_{\mathrm{pe}}$) is:

$$S = \dot{n}_{\mathrm{pe}} = \dot{n}_{\mathrm{a}}\,\eta_{\mathrm{fl}}\,\eta_{\mathrm{ph}}\,\delta$$

where: $\dot{n}_{\mathrm{a}}$ – rate of absorbed photons per second

η_{fl} – quantum efficiency of fluorescence $(\dot{n}_{\mathrm{fl}}/\dot{n}_{\mathrm{a}})$

η_{ph} – quantum efficiency of photocathode $(\dot{n}_{\mathrm{pe}}/\dot{n}_{\mathrm{fl}})$

δ – geometrical collection efficiency

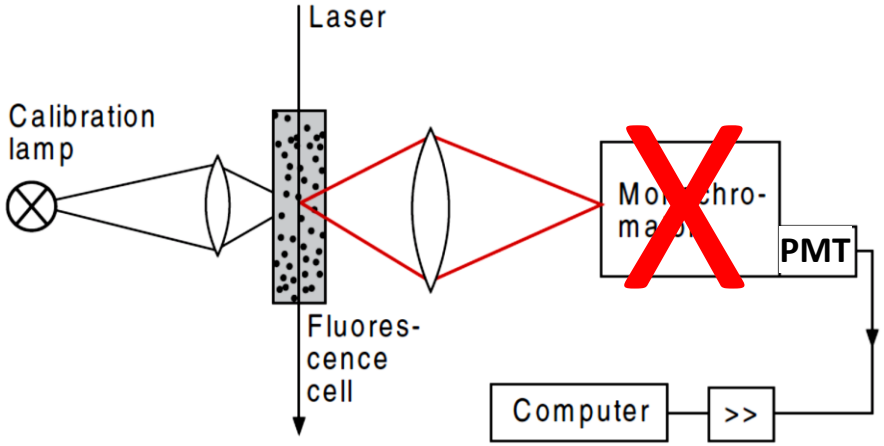

Fig. ref. [1]

Laser induced fluorescence experimental setup

And absorption rate is: $\dot{n}_{\mathrm{a}} = N_k \sigma_{ki} n_{\mathrm{L}} \Delta x$

N_k – number density of molecules in the lower state

σ_{ik} – absorption cross section

n_{L} – number of incident laser photons per second per cm^2

Δx – absorption path length

Achieveble parameters:

η_{ph} = 0.2 (photomultiplier)

δ = 0.1 (solid angle 0.4π)

$\eta_{\mathrm{fl}} \approx 1$

n_{L} = 3 x 10^{18} /s (1 Watt laser at λ=500 nm)

and for

$\dot{n}_{\mathrm{a}}$ = 10^4/s (relative absorption $I_{\mathrm{L}}/I_{\mathrm{L}}$ = 3 x 10^{-15})

photoelectron rate $\dot{n}_{\mathrm{pe}} = 200/\mathrm{s}$

for dark current $\dot{n}_{\mathrm{pe}}(0) = 50/\mathrm{s}$

absorption sensitivity < 10^{-15}

better than any direct absorption technique

Doppler-free spectroscopy in molecular beam

Overcome resolution limit caused by the Doppler width

$$\Gamma_D = \sqrt{\frac{2\ln(2)kT}{mc^2}}\,\nu_0$$

Enables investigation of:

- hyperfine structure
- Zeeman splitting
- rotational structure

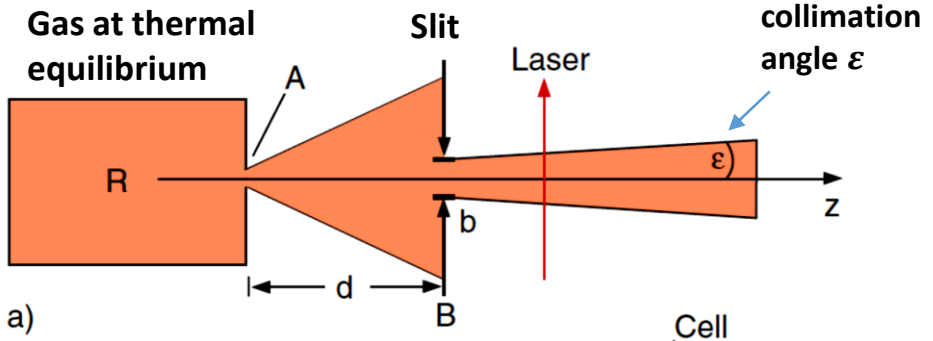

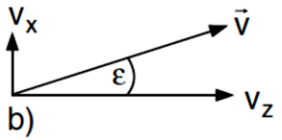

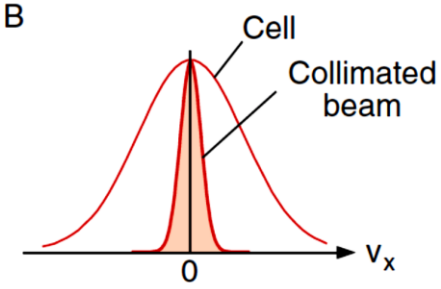

Figs. ref. [1]

Reduced v_x speed in the beam $v_x \le (b/2d)\bar{v} = v_z \tan\varepsilon$

In the beam the density *n* of molecules having speed v within interval $\mathrm{d}v$:

$$n(v, r, \theta) = C\frac{\cos\theta}{r^2} n v^2 \mathrm{e}^{-v/v_p)^2}\,\mathrm{d}v \qquad (*)$$

where $\theta \le \pm\varepsilon$, $r = (z^2 + x^2)^{1/2}$

The absorption line profile:

$$\alpha(\omega, x) = \int n(v_x, x)\sigma(\omega, v_x)\,\mathrm{d}v_x$$

From $v_x = (x/r)v$ and $\cos\theta = z/r$ from eq. (*):

$$n(v_x, x)\,\mathrm{d}v_x = C \cdot n\frac{z}{x^3} v_x^2 \mathrm{e}^{-[(rv_x/xv_p)^2]}\,\mathrm{d}v_x$$

Absorption profile is Lorentzian shape (natural and collisional width) Doppler-shifted by kv_x

$$\sigma(\omega, v_x) = \sigma_0 \frac{(\gamma/2)^2}{(\omega - \omega_0 - kv_x)^2 + (\gamma/2)^2}$$

$v_p = (2kT/m)^{1/2}$ - the most probable velocity

$$n = \int n(v)\,\mathrm{d}v \longrightarrow C = (4/\sqrt{\pi})/v_p^3$$

$$\alpha(\omega) = a \int \frac{e^{-\left[\frac{c(\omega-\omega_0')}{v_p \sin\varepsilon\omega_0'}\right]^2}}{(\omega - \omega_0')^2 + (\gamma/2)^2}\,\mathrm{d}\omega_0' \qquad \omega_0' = \omega_0(1 + v_x/c)$$

Voigt profile with reduced Doppler (Gaussian) width

$$\Delta\omega_D \longrightarrow \Delta\omega_D \sin\varepsilon$$

Doppler-free spectroscopy in molecular beam

Laser-induced fluorescence in molecular beam

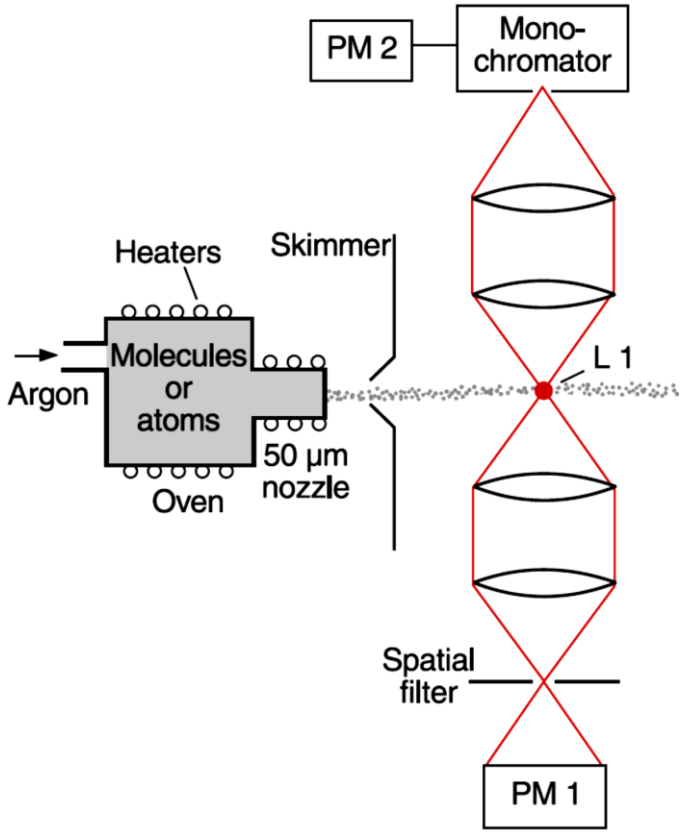

Doppler-limited and Doppler free spectrum of SO_2, (λ ~ 300 nm)

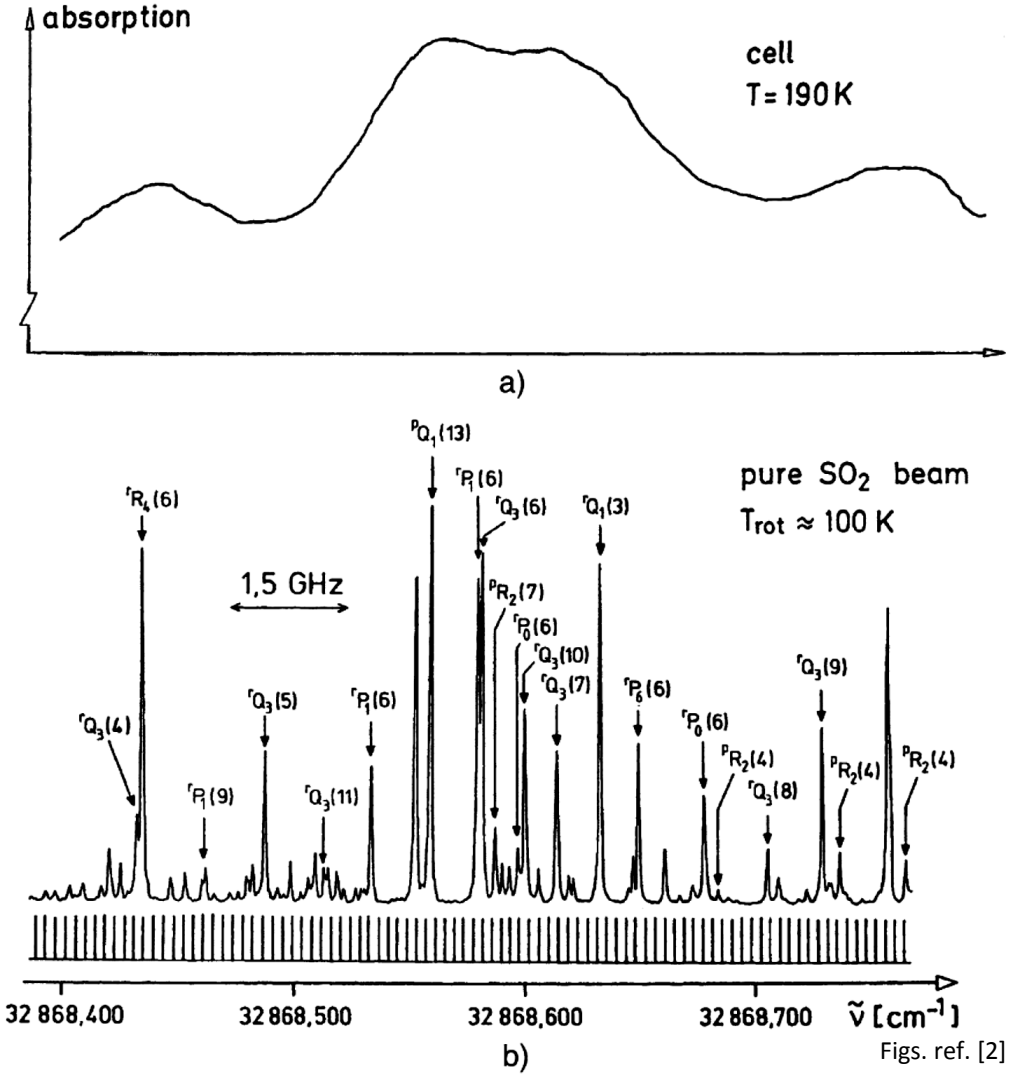

Figs. ref. [2]

Nonlinear absorption spectroscopy

Attenuation *dI* of a plane e-m wave $\mathrm{d}I = -\alpha I\,\mathrm{d}x$
where absorption coeff.

$$\alpha(\omega) = [N_k - (g_k/g_i)N_i]\sigma(\omega) = \Delta N \cdot \sigma(\omega)$$

ΔN – population difference, σ – absorption cross section

$$\mathrm{d}I = -\Delta N \cdot \sigma(\omega) \cdot I \cdot \mathrm{d}x$$

For small *I* population densities N_k, N_i do not depend on *I*

Then α independent of *I* ⟶ Lambert-Beer law $I = I_0\,\mathrm{e}^{-\alpha x} = I_0\,\mathrm{e}^{-\Delta N \sigma x}$

For high *I* : $\mathrm{d}I = -\Delta N(I) \cdot I \cdot \sigma \cdot \mathrm{d}x$ (finite relaxation rate)
Intensity dependent population density (power series expansion)

$$N_k = N_{k0} + \frac{\mathrm{d}N_k}{\mathrm{d}I} I + \frac{1}{2}\frac{\mathrm{d}^2 N_k}{\mathrm{d}I^2} I^2 + \ldots$$

for lower and upper level:

$$\mathrm{d}N_k/\mathrm{d}I < 0 \text{ and } \mathrm{d}N_i/\mathrm{d}I > 0$$

Population difference

$$\Delta N(I) = \Delta N_0 + \frac{\mathrm{d}(\Delta N)}{\mathrm{d}I} I + \frac{1}{2}\frac{\mathrm{d}^2(\Delta N)}{\mathrm{d}I^2} I^2 + \ldots$$

Attenuation

$$\mathrm{d}I = -[\Delta N_0 \sigma I + \frac{\mathrm{d}}{\mathrm{d}I}(\Delta N) I^2 \sigma + \ldots]\,\mathrm{d}x$$

linear **nonlinear**

$\mathrm{d}(\Delta N)/\mathrm{d}I < 0$ - decrease of absorption

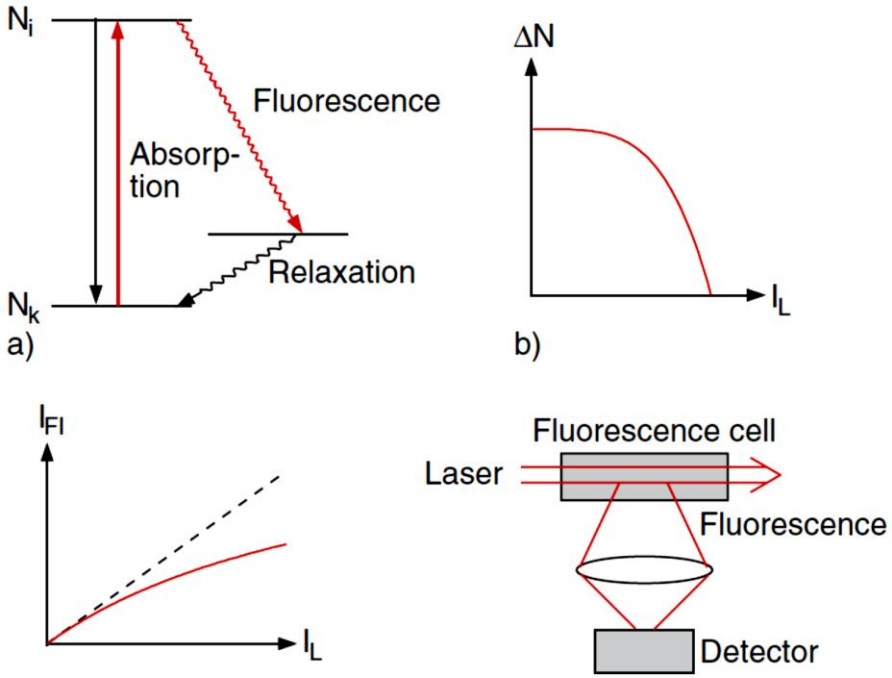

Figs. ref. [1]

Nonlinear absorption can be observed on fluorescence (LIF) signal

Saturation (Doppler free) spectroscopy

- Doppler broadened absorption line centered at ω_0
- laser beam at ω

Doppler shift: $\Delta\omega = kv_x$

only molecules with given velocity may absorb radiation

$$\omega = \omega_0(1 + kv_x)$$

Nonlinear absorption – decrease of $N_k(v_x)$, increase of $N_i(v_x)$

Double pass configuration

decreased absorption at $\omega = \omega_0(1 \pm kv_x)$

at line center doubly decreased absorption – **Lamb dip**

Width of Lamb dip depends on homogeneous line width

- natural width
- collisional broadening

Overlapped Doppler-broadened lines can be resolved

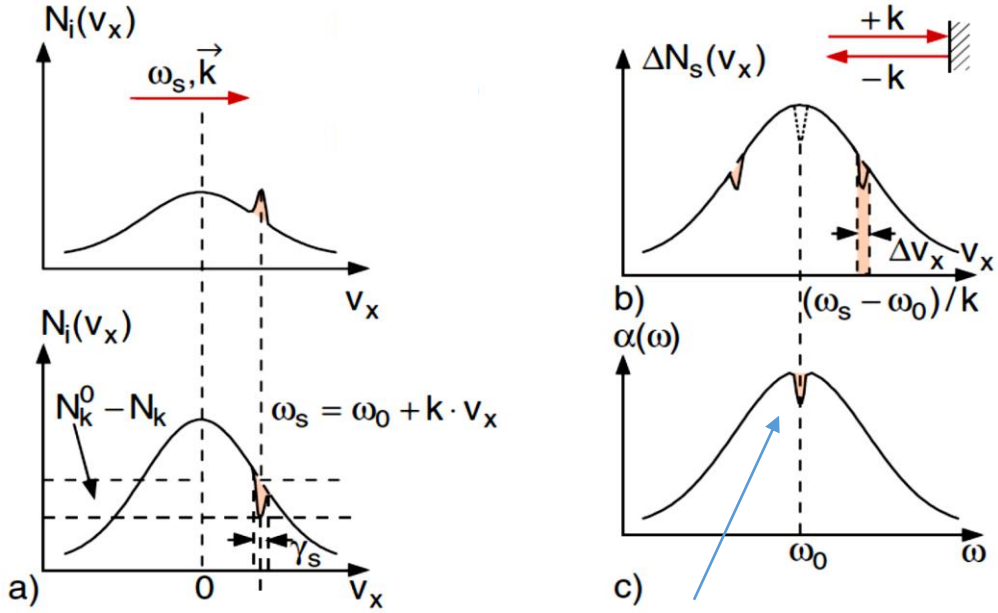

both beams interact with the same group of molecules

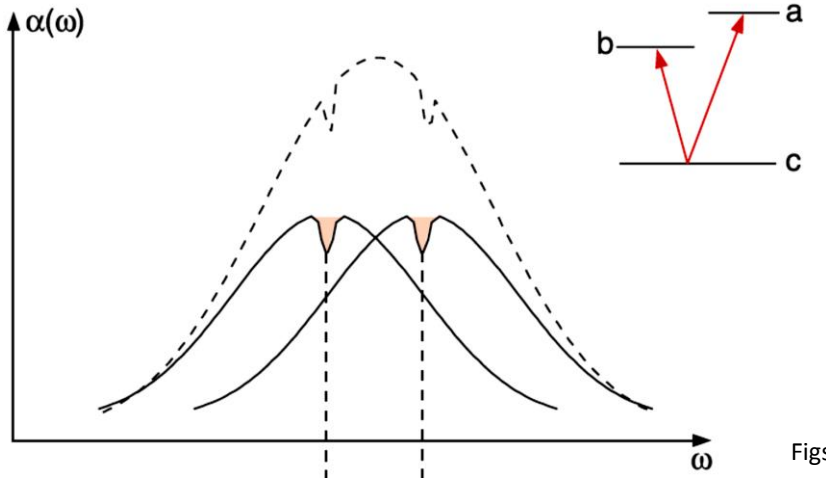

Figs. ref. [1]

Saturation (Doppler free) spectroscopy

Pump and Probe beam configuration:
Doppler-broadened shape can be eliminated

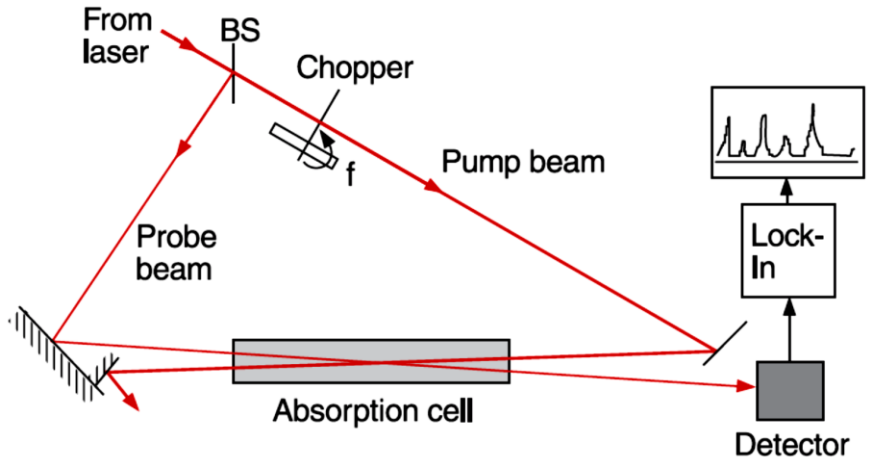

Saturation spectroscopy inside the laser resonator
higher power
standing wave (two directions)

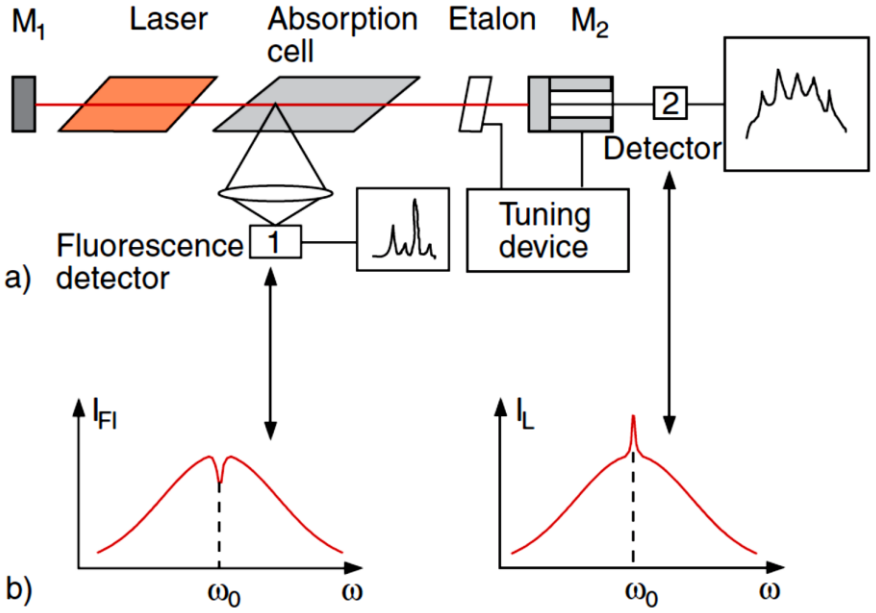

Intracavity FM spectroscopy of I_2 – derivative spectrum
(used for laser frequency stabilization)

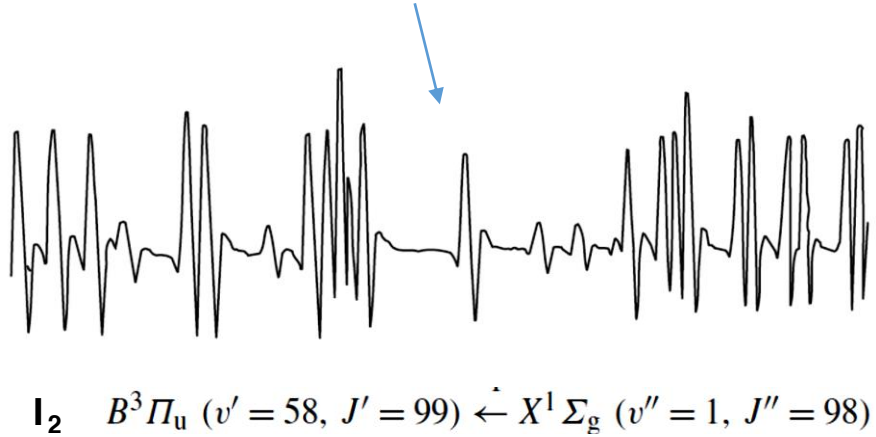

I_2 $B^3\Pi_u\ (v'=58,\ J'=99) \leftarrow X^1\Sigma_g\ (v''=1,\ J''=98)$

Figs. ref. [1]

Doppler-free two-photon spectroscopy

Two photons simultaneously absorbed – induce optical transition with $\Delta L = 0$ or $\Delta L = \pm 2$ depending on two-photon spins

- much weaker than one-photon transitions
- probability enhanced if intermediate level E_m is present

From energy conservation $E_f - E_k = \hbar(\omega_1 + \omega_2)$

For moving molecule - Doppler shift $\omega' = \omega - \boldsymbol{k} \cdot \boldsymbol{v}$

$$E_f - E_k = \hbar(\omega_1 + \omega_2) - \hbar \boldsymbol{v}(\boldsymbol{k}_1 + \boldsymbol{k}_2)$$

For two beams from the same laser with opposite direction

$$\omega_1 = \omega_2 \text{ and } \boldsymbol{k}_1 = -\boldsymbol{k}_2$$

Molecules with all speeds contribute to the Doppler-free two-photon absorption

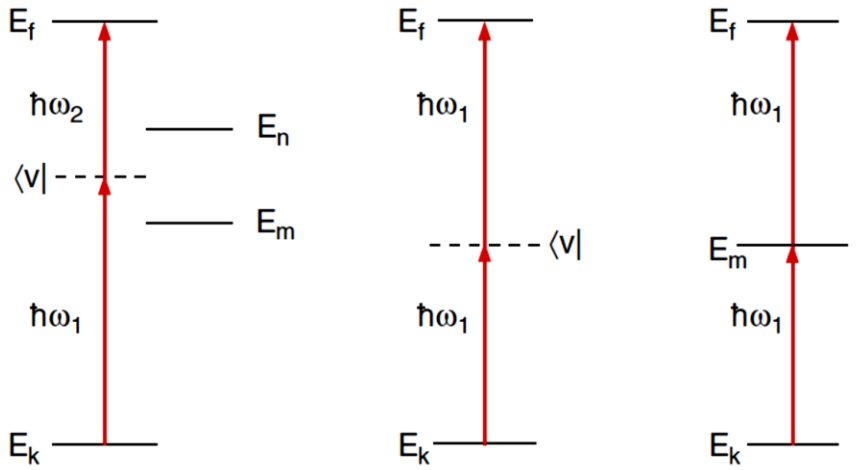

Figs. ref. [1]

Doppler-free two-photon spectroscopy

Experimental setup for two-photon spectroscopy – fluorescence detection

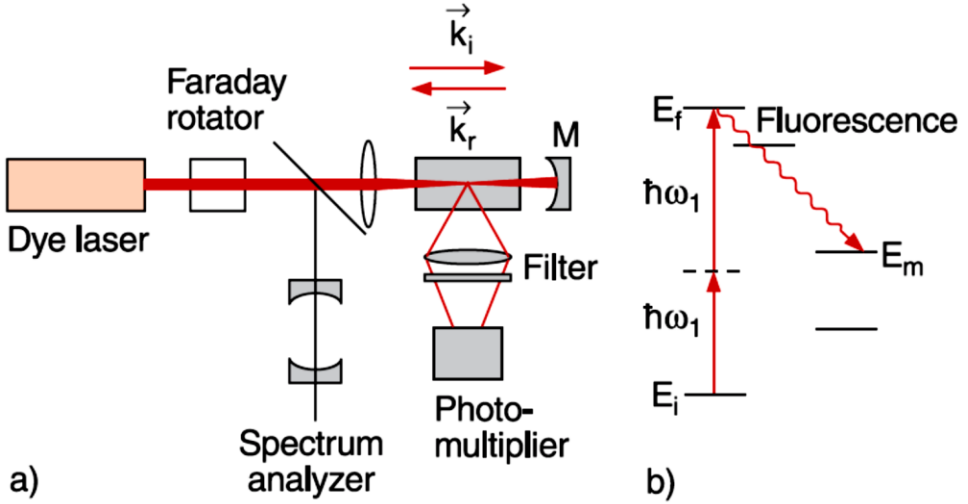

Two photons travelling the same direction (equal ***k***) – Doppler broadened spectrum

Two photons travelling opposite direction (opposite ***k***) – Doppler-free spectrum (two times more probable)

Doppler-free peak is $2 \times \Delta\omega_D / \Delta\omega_n$ times higher than Doppler-broadened background

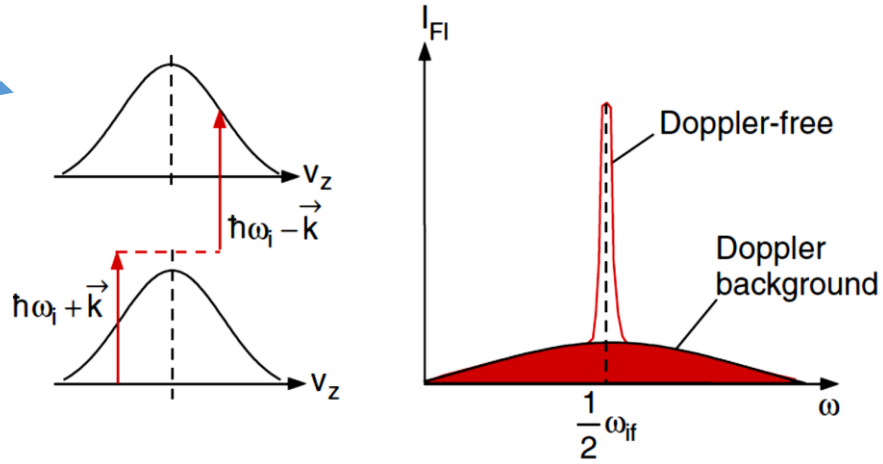

Figs. ref. [1]

Isotope shifts of lead – two-photon spectroscopy

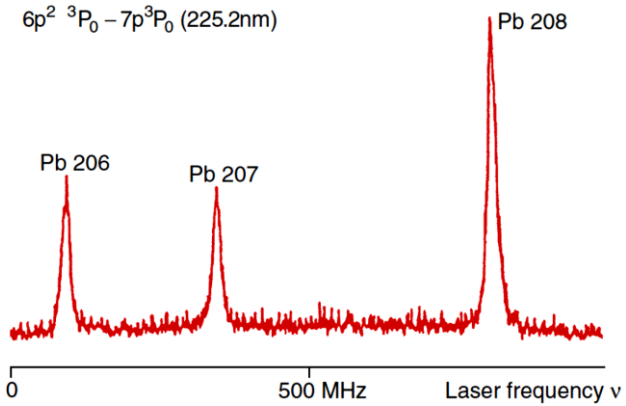

Raman spectroscopy

Inelastic scattering of photons by molecule:

$$\hbar\omega_0 + M(E_k) \rightarrow M^*(E_f) + \hbar\omega_s$$

$$\Delta E = \hbar(\omega_0 - \omega_s) > 0$$ **Stokes radiation**

ΔE corresponds to vibrational, rotational or electronic energy of the molecule

Super elastic scattering on excited molecule:

$$\Delta E = \hbar(\omega_0 - \omega_a) < 0$$ **anti-Stokes radiation**

Resonance Raman effect – if a virtual state ⟨v| coincides with one of real molecular eigenstate

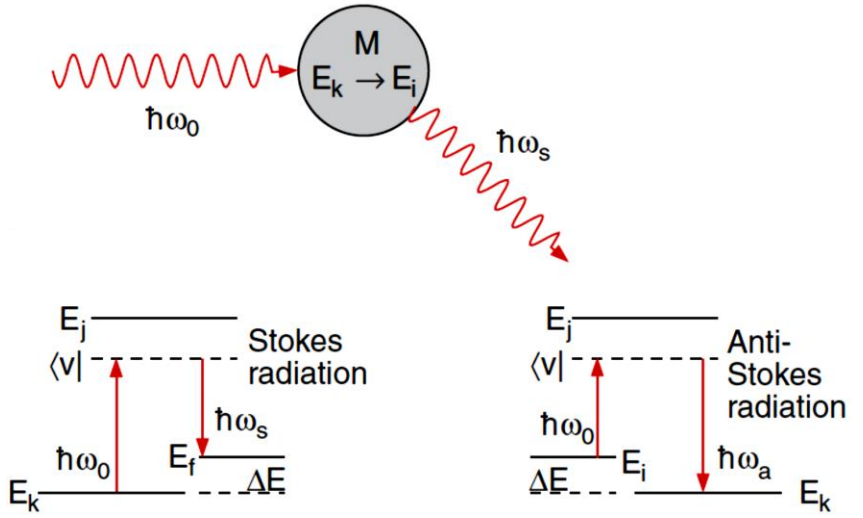

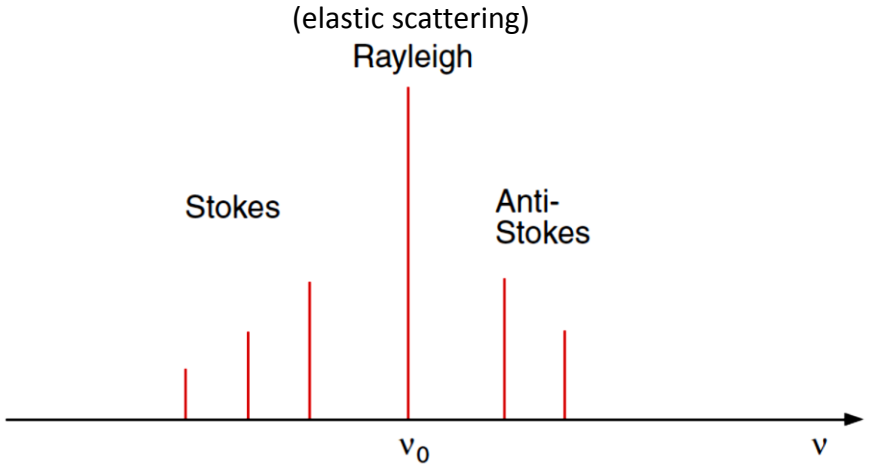

Schematic Raman spectrum

Figs. ref. [1]

Raman spectroscopy

Classical description

Electric dipole moment of molecule:

$$\boldsymbol{p}(E) = \boldsymbol{p}_0 + \tilde{\alpha}\boldsymbol{E} \qquad (*)$$

($\boldsymbol{p}_0$: permanent; $\tilde{\alpha}\boldsymbol{E}$: induced)

$\boldsymbol{p}$ and $\tilde{\alpha}$ depends on nuclear displacements q_n of the vibrating molecule

For small displacements q – expansion to Taylor series:

$$\boldsymbol{p}(q) = \boldsymbol{p}(0) + \sum_{n=1}^{Q}\left(\frac{\partial \boldsymbol{p}}{\partial q}\right)_0 q_n + \ldots \qquad \alpha_{ij}(q) = \alpha_{ij}(0) + \sum_{n=1}^{Q}\left(\frac{\partial \alpha_{ij}}{\partial q_n}\right)_0 q_n$$

n-th normal vibration: $q_n(t) = q_{n0}\cos(\omega_n t)$

electric field amplitude: $\boldsymbol{E}(t) = \boldsymbol{E}_0 \cos \omega t$

From eq. (*):

$$\boldsymbol{p}(t) = \boldsymbol{p}_0 + \sum_{n=1}^{Q}\left(\frac{\partial \boldsymbol{p}}{\partial q_n}\right)_0 q_{n0}\cos(\omega_n t) + \alpha_{ij}(0)\boldsymbol{E}_0 \cos \omega t$$

$$+ \frac{1}{2}\boldsymbol{E}_0 \sum_{n=1}^{Q}\left(\frac{\partial \alpha_{ij}}{\partial q_n}\right)_0 q_{n0}[\cos(\omega+\omega_n)t + \cos(\omega-\omega_n)t]$$

permanent dipole moment

infrared spectrum intensity $\sim \partial \boldsymbol{p}/\partial q_n$

Rayleigh scattering

Raman scattering intensity $\sim \partial \alpha/\partial q_n$

Infrared and Raman spectroscopy supplement each other

$\tilde{\alpha}$ - electric polarizability (tensor $[\alpha_{ij}]$)

Q – number of normal vibrational modes of molecule
(3N-6 or 3N-5 for linear molec.)

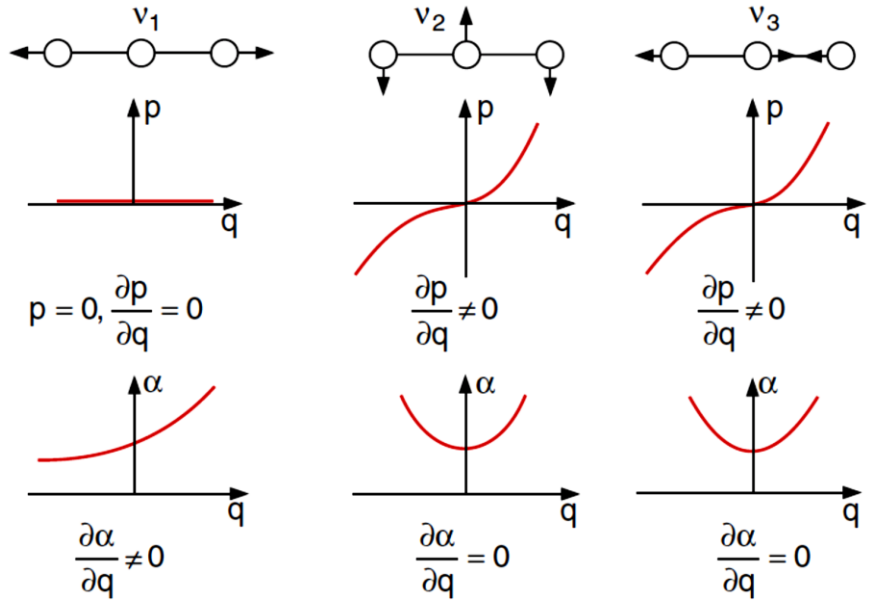

Figs. ref. [1]

Normal vibrations of CO_2 molecule:
ν_1 – Raman spectrum, ν_2, ν_3 – infrared spectrum

Cavity-enhanced laser absorption spectroscopy

Optical cavity is used to

- **increase absorption path length**

  effective path length $L_{\text{eff}} = L/(1 - R + A)$

  A – all other losses except for transmission

- separate frequencies – **increase resolution**
- **increase radiation power**

  e.g. saturation effects

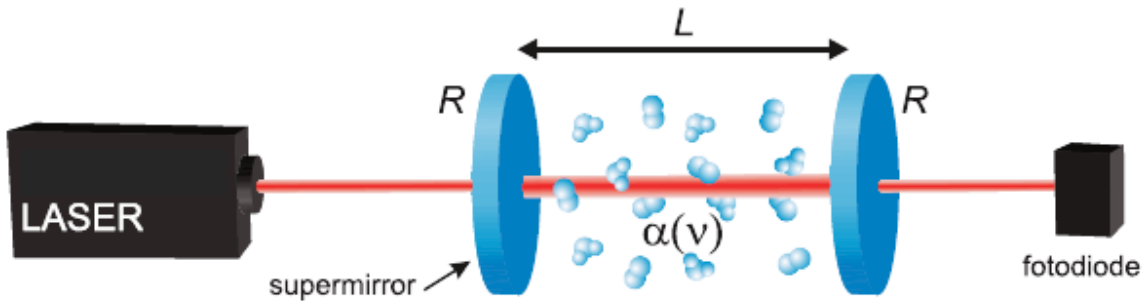

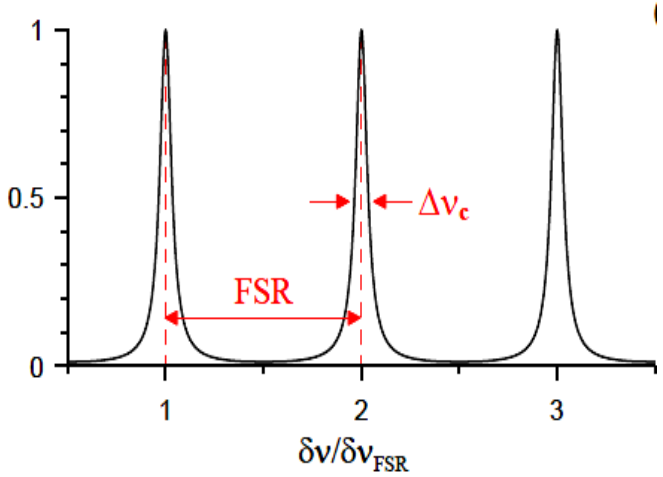

Absorbing medium inside the cavity

Near resonance transition, absorption and dispersion of the field *E(t,z)* is described by the imaginary and real part of the complex refractive index:

$$n_a(\nu) = n'(\nu) - i\kappa(\nu)$$

The electric field in the medium having an optical resonance:

$$E(t,z) = E_0\, e^{-k\kappa(\nu)z}\, e^{i\{2\pi\nu t - k[n+n'(\nu)-1]z\}}$$

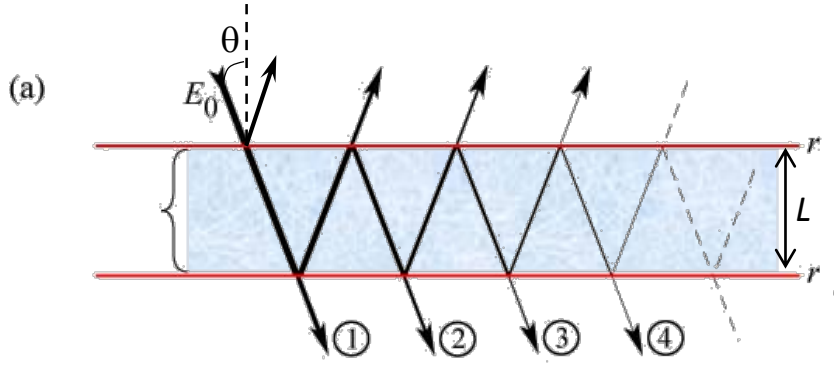

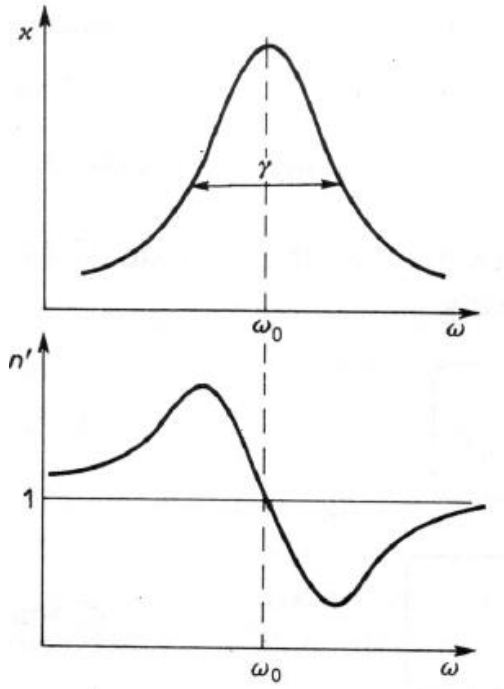

related to each other by Kramers-Kronig equations

W. Demtröder „Laser spectroscopy"

Transmitted field:

$$E_T = t^2 E_0\, e^{-k\kappa(\nu)L}\, e^{i\{2\pi\nu t - k[n+n'(\nu)-1]L\}} \frac{1}{1 - r^2\, e^{-2k\kappa(\nu)L}\, e^{-i2k(n+n'(\nu)-1)L}}$$

Transmitted intensity (modified Airy equation):

$$I_T(\nu) = I_0 \frac{(1-R)^2\, e^{-\alpha(\nu)L}}{(1-R\,e^{-\alpha(\nu)L})^2} \frac{(1-R\,e^{-\alpha(\nu)L})^2}{(1-R\,e^{-\alpha(\nu)L})^2 + 4R\,e^{-\alpha(\nu)L} \sin^2\left(\frac{\pi\nu}{\nu_{FSR}(\nu)}\right)}$$

$$\nu_{FSR}(\nu) = c/[2L(n+n'(\nu)-1)]$$

Consequences of gas absorption in the cavity

- The presence of absorbing medium modifies properties of the cavity
- As a result of refractive index changes in the vicinity of molecular transition cavity modes are broadened and shifted
- Dependence of FSR on frequency can be calculated on the base of Kramers-Krönig realtion for the real and imaginary parts of the complex refractive index

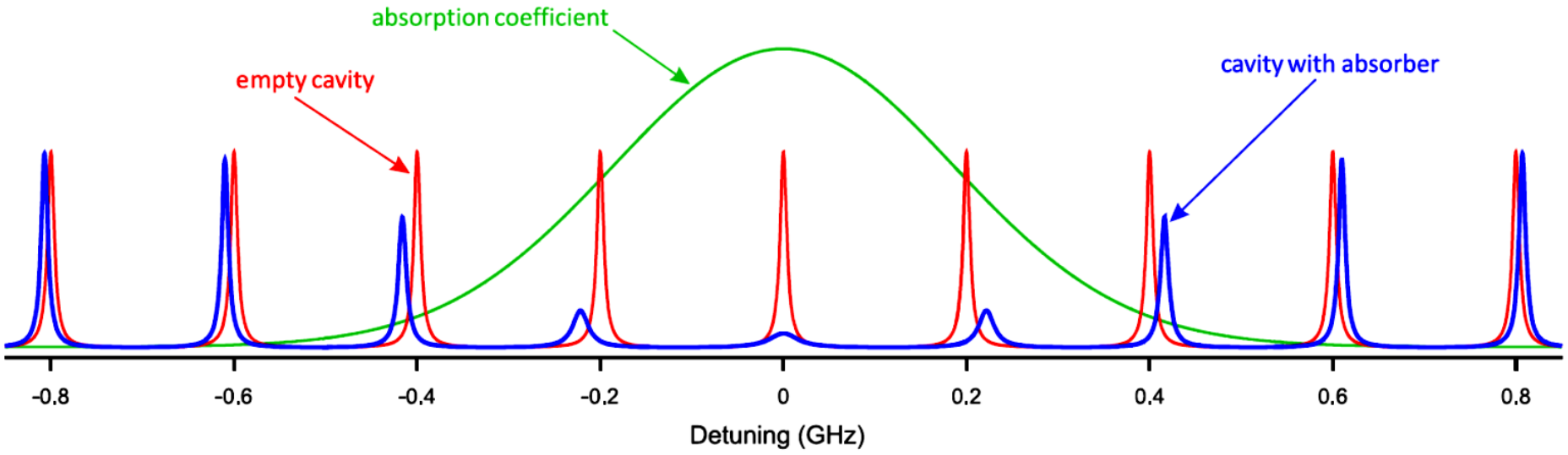

Cavity ring-down spectroscopy

After the first impulse pass through the cavity

$$I_0^{(\mathrm{imp})}(\nu) = T^2 I_{\mathrm{las}}(\nu) e^{-\alpha(\nu)L},$$

Next impulse decreased by $R^2 exp(-2\alpha(\nu)L)$

$$I_N^{(\mathrm{imp})}(\nu) = I_0^{(\mathrm{imp})}(\nu) R^{2N} e^{-2N\alpha(\nu)L}$$

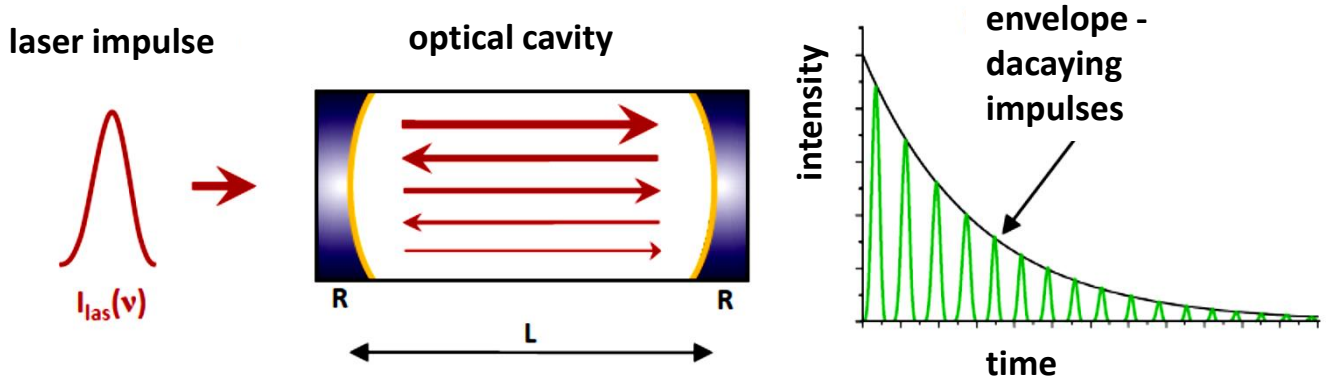

For continuous-wave laser

$$I(\nu,t) = I_0(\nu)\left(R\, e^{-\alpha(\nu)L}\right)^{ct/L}$$

$$I(\nu,t) = I_0(\nu) e^{(\ln(\mathrm{R})-\alpha(\nu)L)ct/L} = I_0(\nu)\exp(-t/\tau(\nu))$$

Time constant of the light decay:

$$\tau(\nu) = \frac{L}{c(-\ln(R) + \alpha(\nu)L)}$$

Assuming that $\ln(R) \approx R - 1$

$$\alpha(\nu) = \frac{1}{c}\left(\frac{1}{\tau(\nu)} - \frac{1}{\tau_0}\right) \qquad \tau_0 = \frac{L}{c(1-R)}$$

Decay time const. for empty cavity

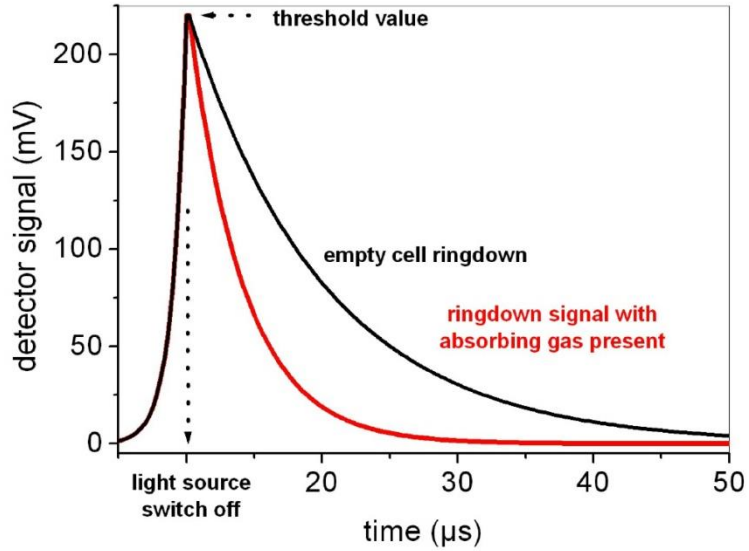

Spectral line shape and line intensity

line shape — number density

$$\int I(\nu)d\nu = cSn$$

speed of light — intensity

→ remote sensing
→ Doppler thermometry
→ determination of physical constants
→ isotope ratio measurements
→ verification of molecular interactions potentials

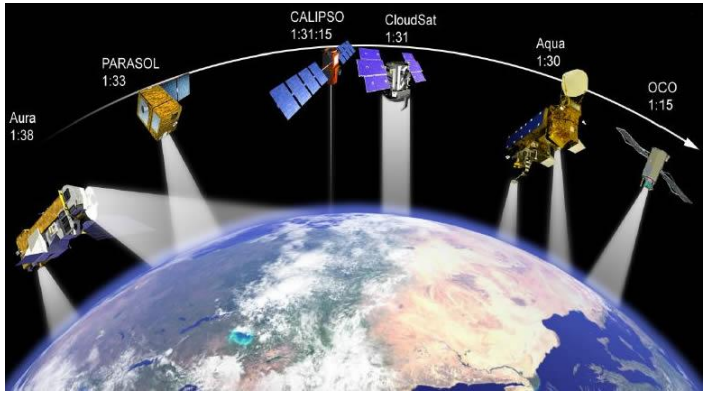

Satellite remote sensing accuracy requirements: **<1%**
<0.3% (for CO_2 variations)

Database accuracy: **~2-4%** (intensity)
e.g. O_2 B band **~300 MHz** (line position HITRAN08)
~50 MHz (line position HITRAN12)

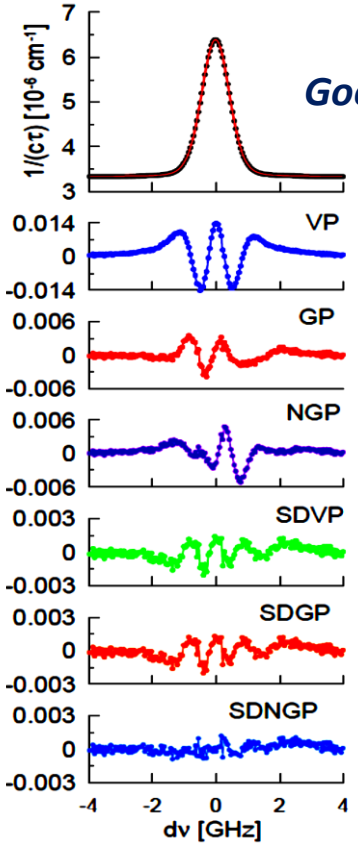

Good knowledge of the line shape

- ✓ pressure and Doppler broadening
- ✓ speed-dependent effects
- ✓ Dicke narrowing
- ✓ phase- and velocity-changing collisions correlations
- ✓ …

Good performance of an experiment

- ✓ **high spectral resolution**
- ✓ **high precision**
- ✓ **high accuracy**
- ✓ **wide dynamic range of measurements**
- ✓ **high speed of data acquisition**
- ✓ **very stable frequency axis**
- ✓ **…**

Pressure and temperature dependence of spectral line shapes

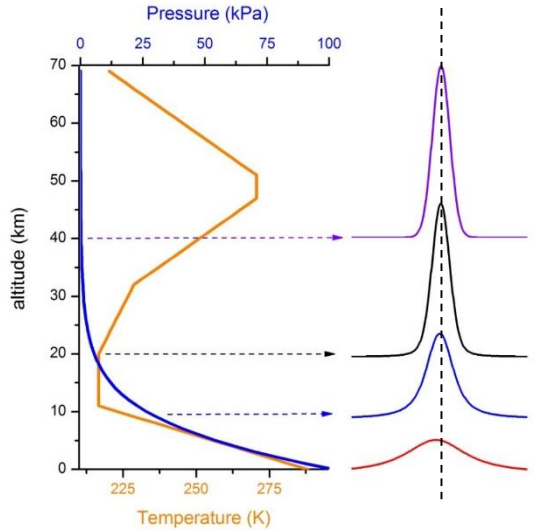

Important parameters: line position, width, shift, intensity, …

Spectral line shape and line intensity

line shape

number density

$$\int I(\nu)d\nu = cSn$$

speed of light

intensity

Systematic error of line intensity determination caused by simplified line shape model

- Voigt profile (VP) – several percent error
- Hartmann-Tran profile (HTP) < 0.1 percent error
- HTP – recommended for new generation of spectroscopic databases
- **Experimental accuracy ~ 0.1 % is a challenge**

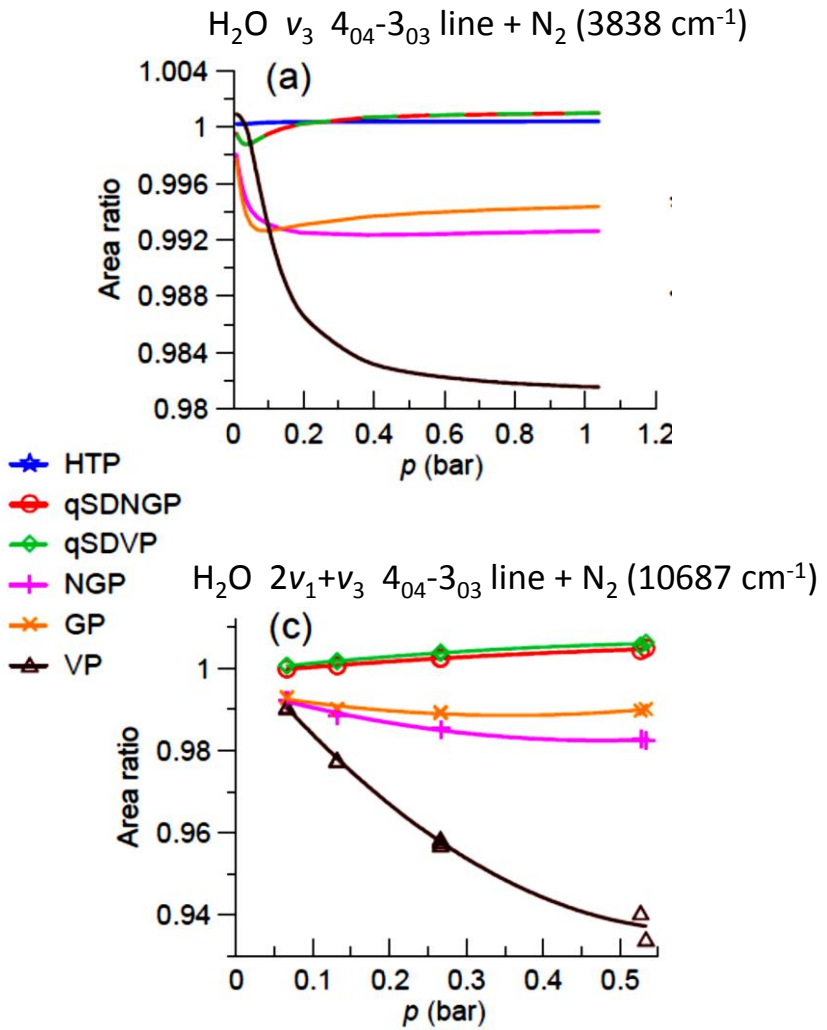

N.H. Ngo et al. JQSRT **129**, 89 (2013)
J. Tennyson et al. *Pure Appl. Chem*. **86**, 1931 (2014)

D. Lisak et al. *JQSRT* (2015)
doi: 10.1016/j.jqsrt.2015.06.012

Cavity ring-down spectroscopy

Excitation of the optical cavity with short laser pulse, having various spectral widths $\Delta\nu_p$

Exp. decay for $\Delta\nu_p << \Delta\nu_{FSR}$

$\Delta\nu_{FSR}$ – cavity free spectra range

Single-mode CRDS

Multi-mode CRDS

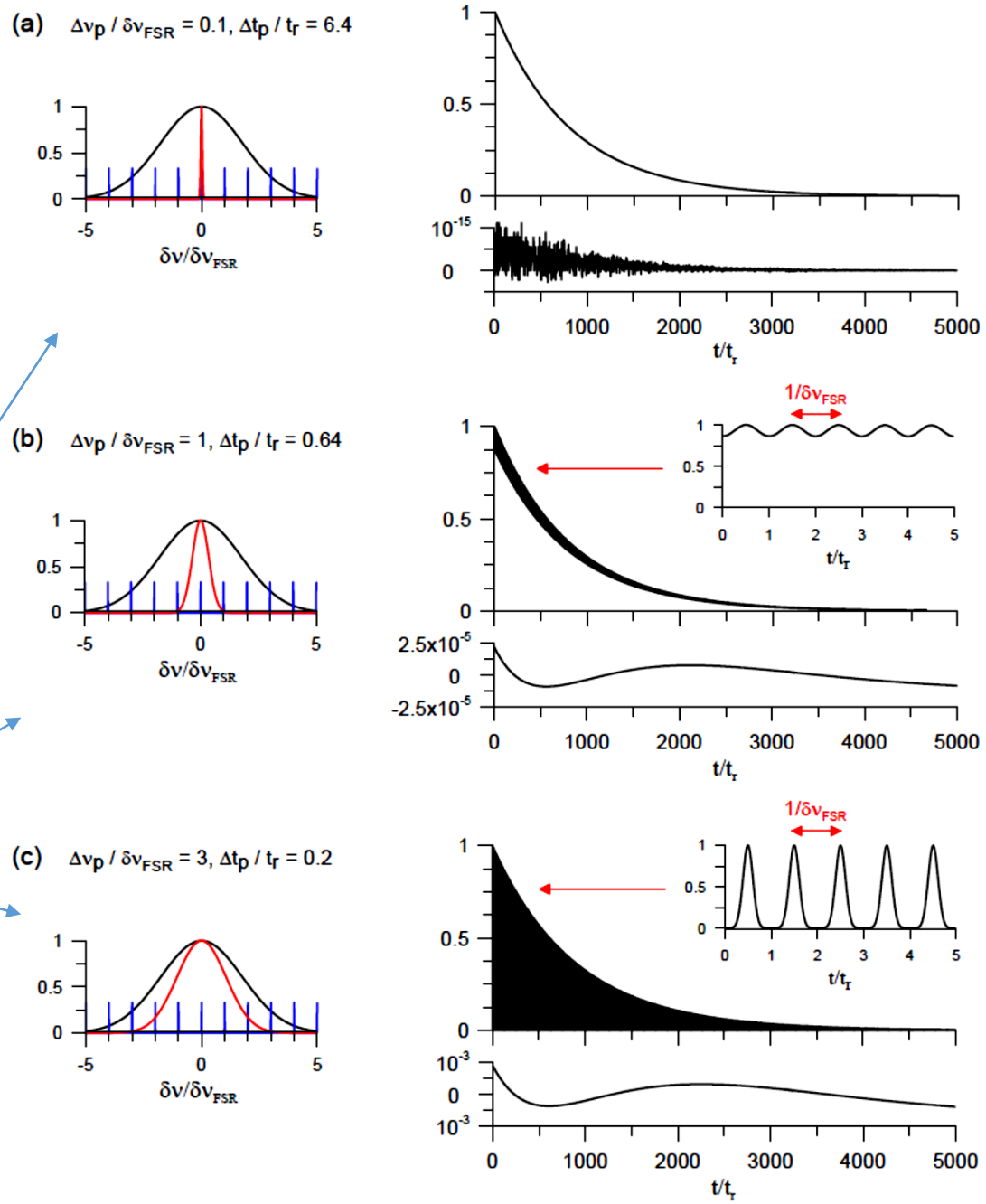

Transverse modes of the optical cavity

Transverse modes may have different decay times

- different optical frequency
- different mirror losses & diffraction

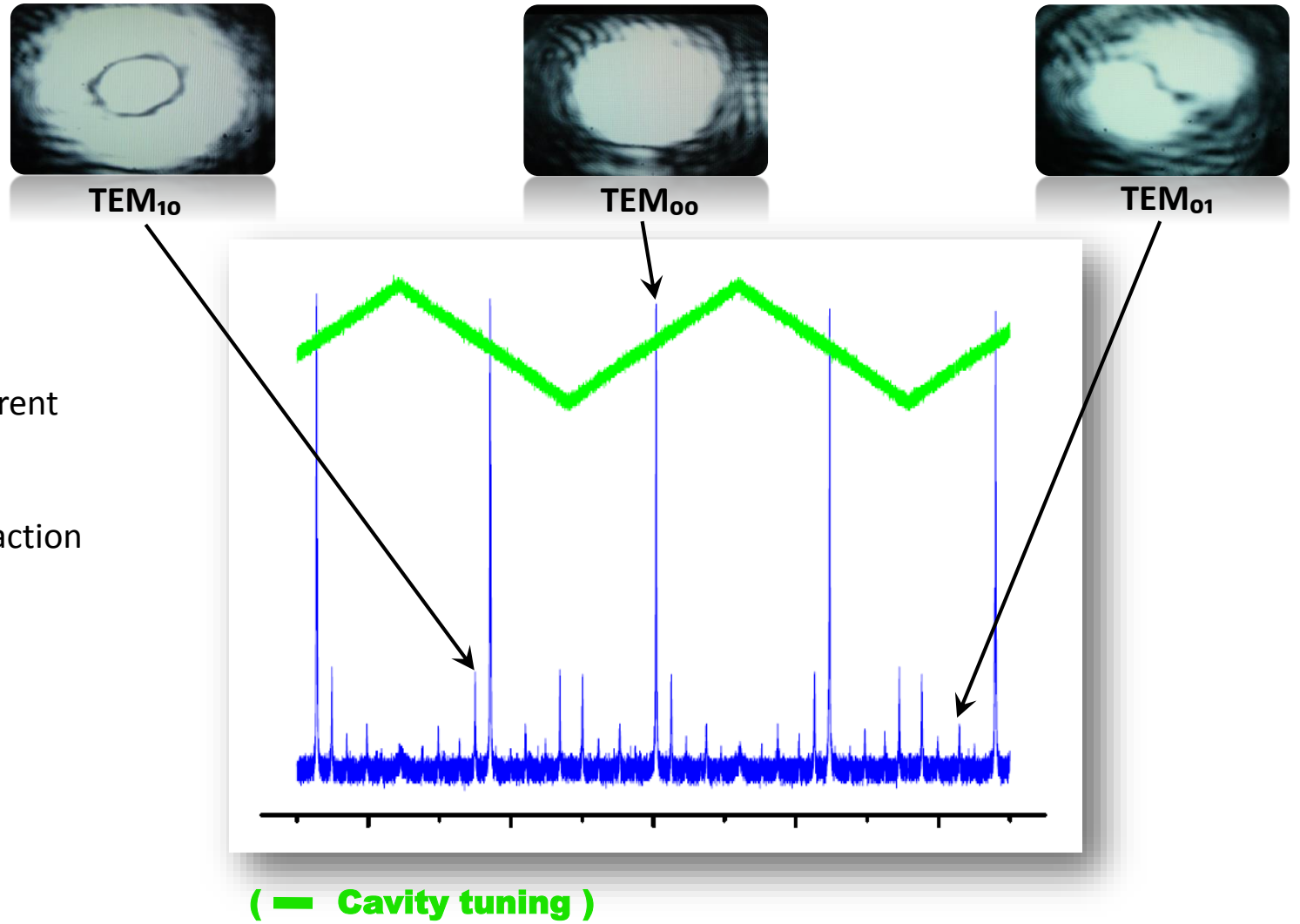

Modes of the optical cavity

Gauss – Hermite modes:

$$\nu_{lmn} = \frac{\omega_{lmn}}{2\pi} = \frac{c}{2L}\left[l + \frac{2}{\pi}(m+n+1)\,\mathrm{arc\,tg}\left(\frac{L}{\sqrt{L(2r-L)}}\right)\right]$$

L – distance between mirrors
r – mirror radius of curvature

longitudinal modes

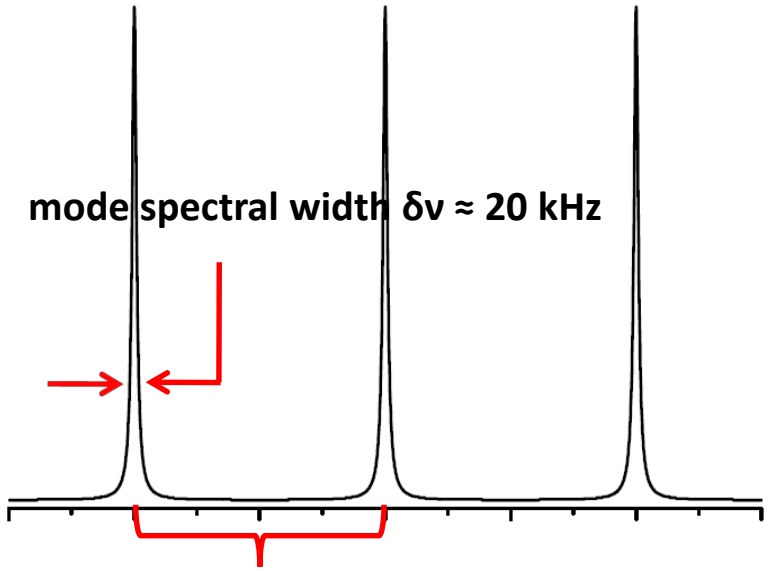

FSR ≈ 200 MHz (R ≈ 0.9997%)

Transverse e-m modes TEM_{mn}

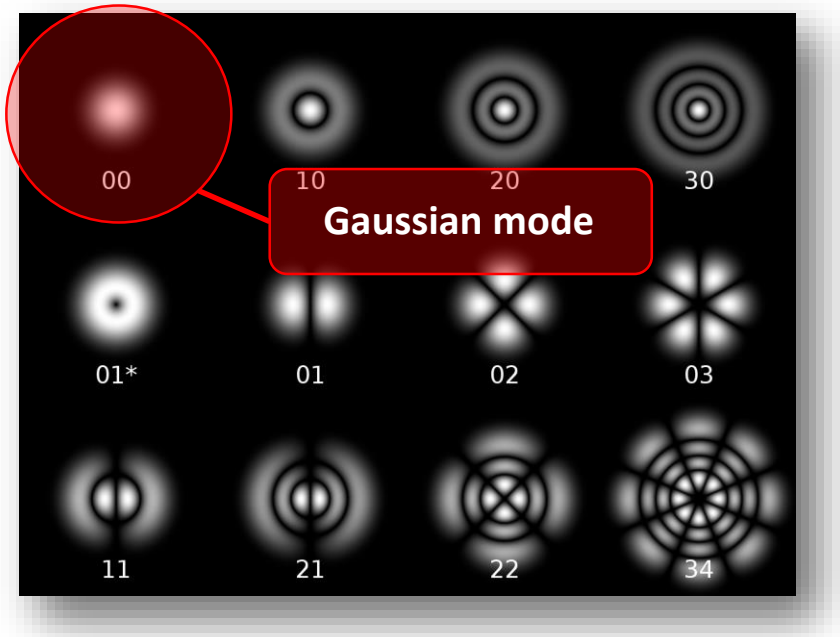

Mode-matching

Gaussian beam

$$E = E(x, y, z, \omega, t) = U(x, y, z)e^{-i(\omega t - kz)}$$

From the wave equation $\Delta E + k^2 E = 0$
we get modes $U_{mn}(x,y,z)$.

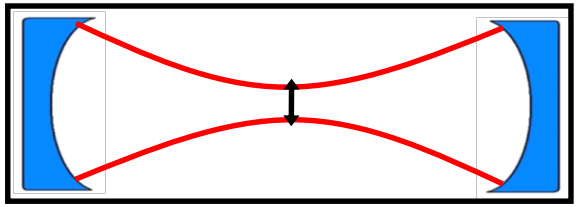

concave-mirror cavity

$$r' = \sqrt{x^2 + y^2}$$

$\varphi(z)$ is a complex phase shift

Gaussian mode

$$U(x, y, z) = e^{-i\left(\varphi(z) + (k/2q)r'^2\right)}$$

$$U(x, y, z) = e^{-r'^2/w(z)^2} e^{-i\left((kr'^2/R'(z)) - i\varphi(z)\right)}$$

$$\frac{1}{q} = \frac{1}{R'} - i\frac{2}{kw^2}$$

From the wave equation

$$\frac{dq}{dz} = 1, \qquad \frac{d\varphi}{dz} = -\frac{i}{q}$$

$$R'(z = 0) = \infty$$

$$q = q_0 + z = i\frac{kw_0^2}{2} + z$$

Width and radius of curvature of Gaussian beam

$$w(z) = w_0\sqrt{1 + \left(\frac{2z}{kw_0^2}\right)^2}$$

$$R'(z) = z\left[1 + \left(\frac{kw_0^2}{2z}\right)^2\right]$$

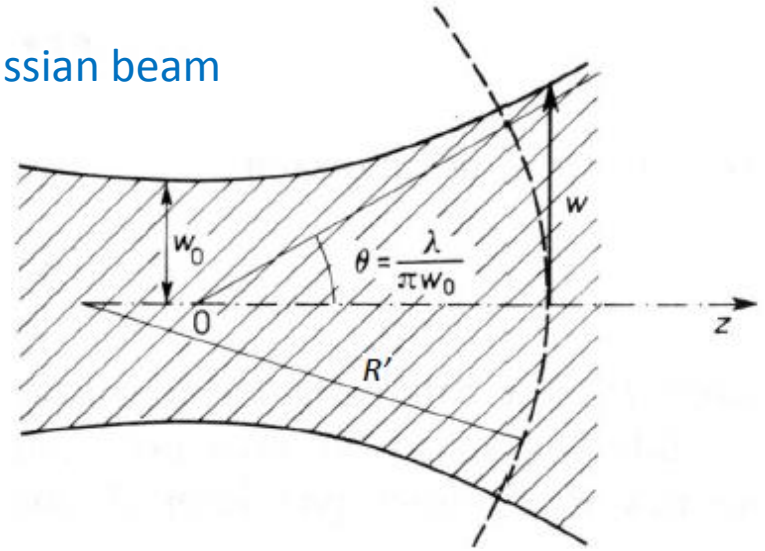

Mode-matching of laser to cavity

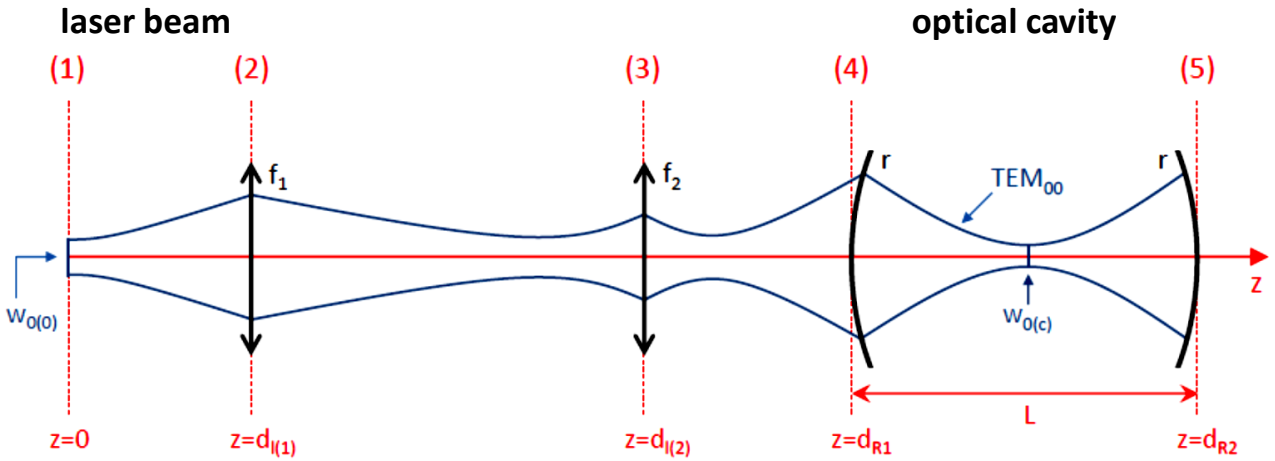

ABCD matrix formalism for Gaussian beam

$$\begin{pmatrix} q_2 \\ 1 \end{pmatrix} = k \begin{pmatrix} A & B \\ C & D \end{pmatrix} \begin{pmatrix} q_1 \\ 1 \end{pmatrix}$$

$$k = 1/(Cq_1 + D)$$

$$\frac{1}{q} = \frac{1}{R'} - i\frac{2}{kw^2}$$

Gaussian profile of TEM_{00} mode

$$w_{0(c)}^2 = \frac{\sqrt{L(2r-L)}}{k}$$

$$R'(z) = z\left[1 + \left(\frac{kw_0^2}{2z}\right)^2\right]$$

(1) initial Gaussian beam measurement

$$\begin{pmatrix} q_{(1)} \\ 1 \end{pmatrix} = \begin{pmatrix} ikw_{0(0)}^2/2 \\ 1 \end{pmatrix}$$

(2) Translation to distance $d_{I(1)}$

$$\begin{pmatrix} q_{(2)} \\ 1 \end{pmatrix} = \begin{pmatrix} 1 & d_{I(1)} \\ 0 & 1 \end{pmatrix} \begin{pmatrix} q_{(1)} \\ 1 \end{pmatrix}$$

(3) Transition through lens f_1 and translation by d_{23}

$$\begin{pmatrix} q_{(3)} \\ 1 \end{pmatrix} = \begin{pmatrix} 1 - d_{23}/f_1 & d_{23} \\ -1/f_1 & 1 \end{pmatrix} \begin{pmatrix} q_{(2)} \\ 1 \end{pmatrix}$$

(4) Transition through lens f_2 and translation by d_{34}

$$\begin{pmatrix} q_{(4)} \\ 1 \end{pmatrix} = \begin{pmatrix} 1 - d_{34}/f_2 & d_{34} \\ -1/f_2 & 1 \end{pmatrix} \begin{pmatrix} q_{(3)} \\ 1 \end{pmatrix}$$

(5) Transition through the cavity mirror with curvature radius r and translation by d_{45}

$$\begin{pmatrix} q_{(5)} \\ 1 \end{pmatrix} = \begin{pmatrix} 1 + 2L/r & L \\ 2/r & 1 \end{pmatrix} \begin{pmatrix} q_{(4)} \\ 1 \end{pmatrix}$$

Mode-matching of laser to cavity

He-Ne laser

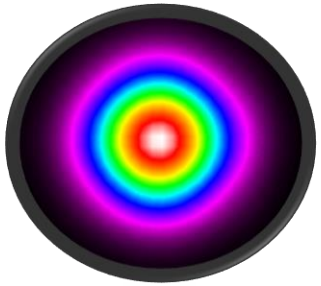

Diode lasers may have strongly non-Gaussian beam shapes

Transmission through a single-mode fiber will clean the beam shape (and decrease power)

Diode lasers

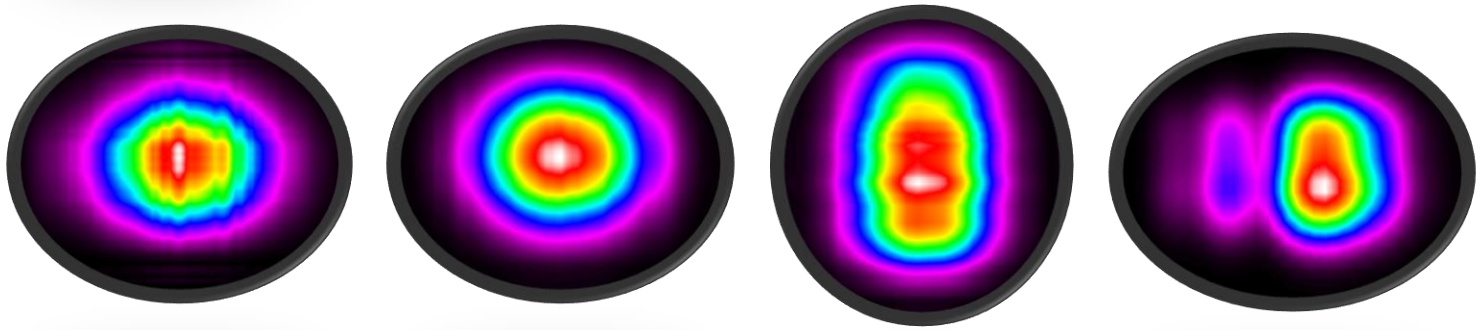

Cavity ring-down spectroscopy - CRDS

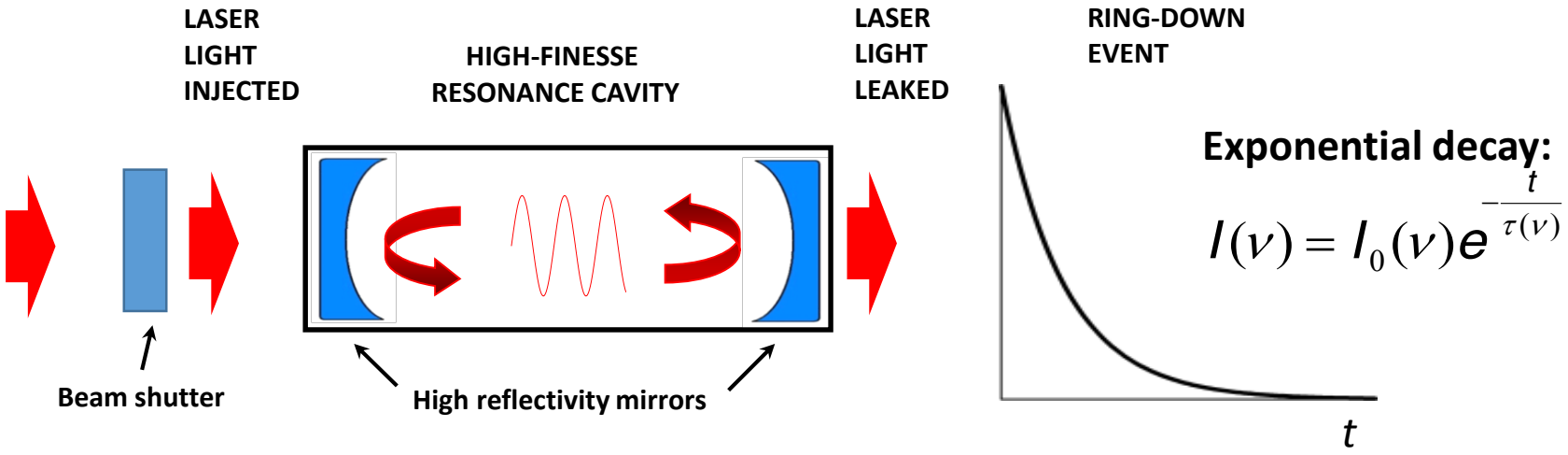

Exponential decay:

$$I(\nu) = I_0(\nu) e^{-\frac{t}{\tau(\nu)}}$$

Decay time

$$\tau(\nu) = \frac{L}{c(1 - R + \alpha(\nu) L)}$$

$$[c\,\tau(\nu_q)]^{-1} = \alpha_{bg}(\nu_q) + \alpha_{\text{abs}}(\nu_q)$$

$$= \alpha_{bg}(\nu_q) + nc \sum_i S_i g_i(\nu_q - \nu_i),$$

$$\delta\nu_m(\nu) \approx \frac{1}{2\pi n \tau(\nu)}$$

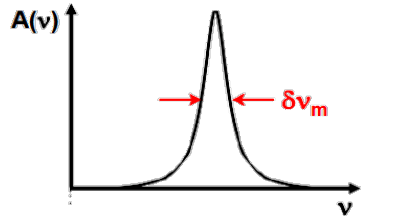

- **high sensitivity** (long optical path)
- **high spectral resolution** (cavity filters frequencies)
- **insensitive to laser power fluctuations** (time is measured)
- **self-calibrated absorption** (no cavity *L* needed to measure α)

Frequency-stabilized cavity ring-down spectroscopy FS-CRDS

Vibrations and thermal drift of cavity resonances

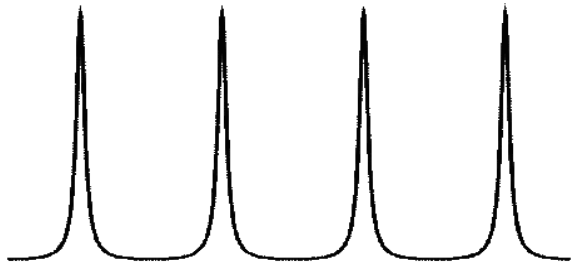

FS-CRDS * → ***Frequency-Stabilized CRDS***

Active stabilization of the optical path length in the cavity

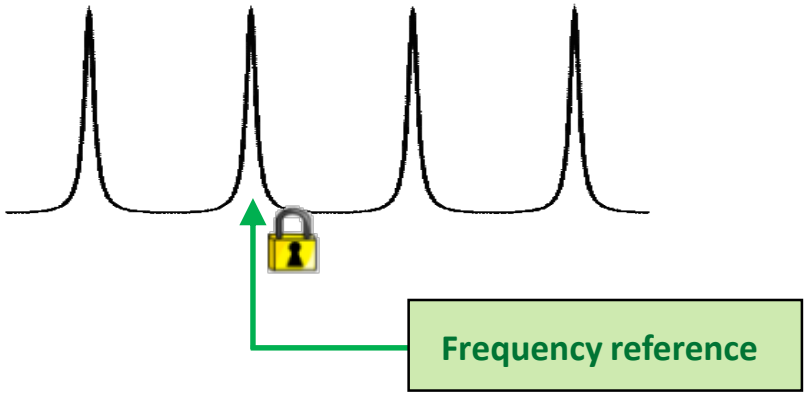

Hodges, Layer, Miller, Scace, *Rev. Sci. Instrum.* **75**, 849 (2004).

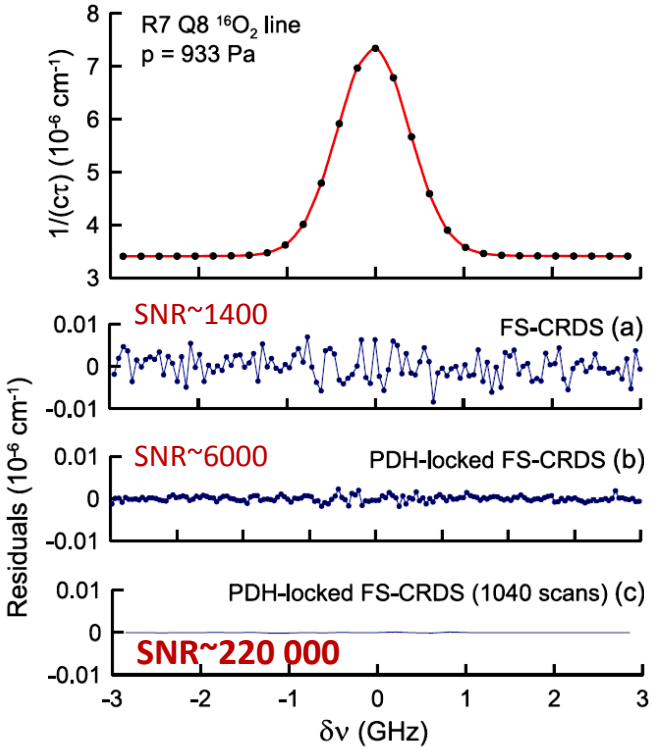

A. Cygan, et al., *Phys. Rev. A.* **85**, 022508 (2012)

Experimental setup for FS-CRDS

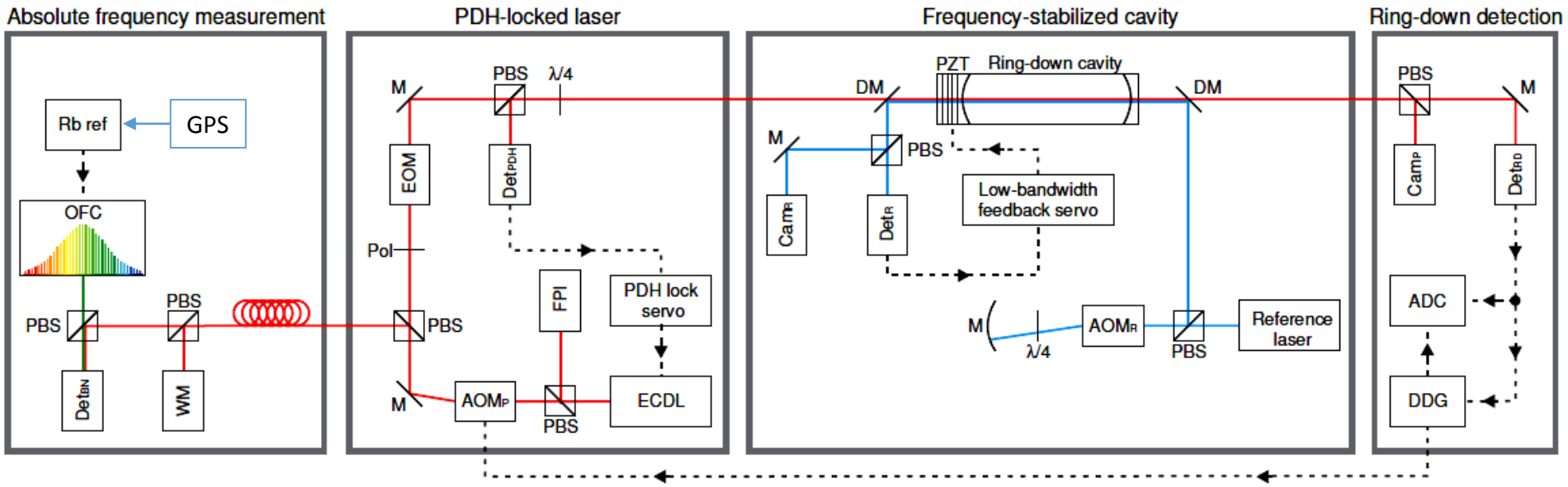

resolution ≈ 1 MHz to 10 kHz depending on the reference laser

3000 decays in 0.2 s, f_{rep} = 15 kHz

Detection limit of absorption coefficient

$$\frac{\alpha_{\min}}{\sqrt{f_{rep}}} \approx 7.5 \times 10^{-11}\ \mathrm{cm}^{-1}\ \mathrm{Hz}^{-1/2}$$ (with 300 ppm mirrors)

Locking the laser to cavity mode with Pound-Drever-Hall (PDH) scheme

Fast phase modulation (with EOM)

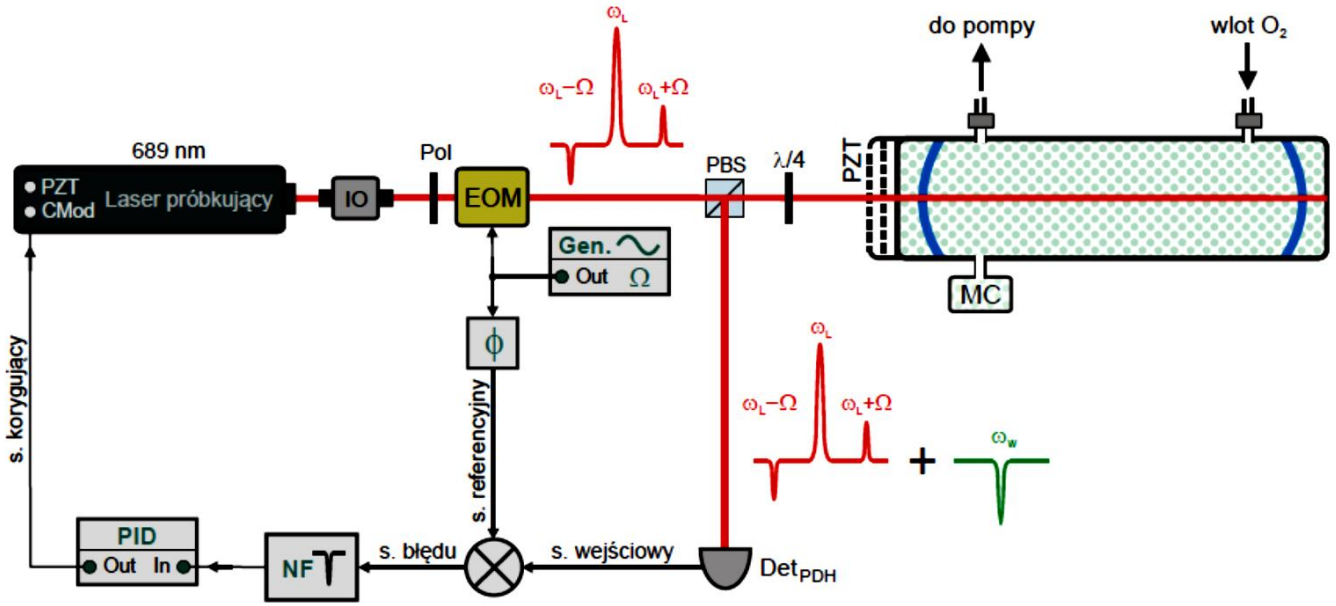

PDH lock setup

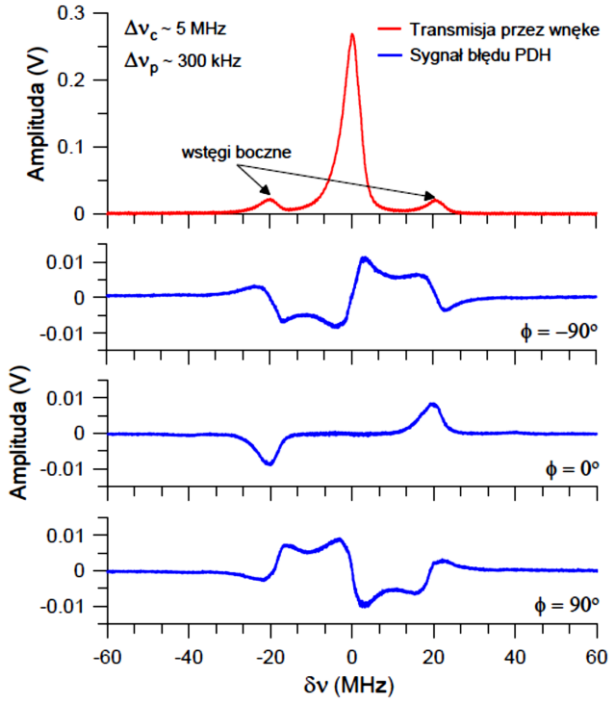

Transmission and PDH error signal
PDH vs phase of the reference signal

Laser lock to the cavity

low-bandwidth lock

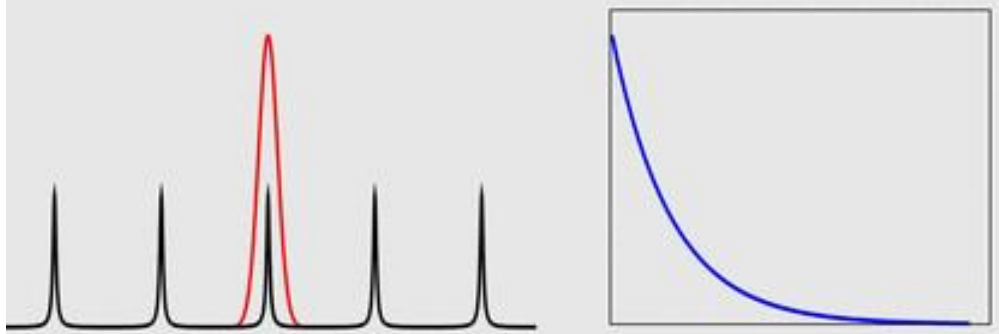

high-bandwidth Pound-Drever-Hall lock

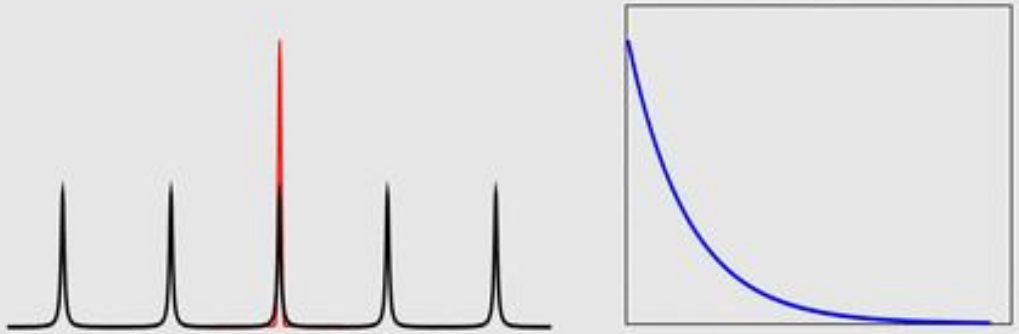

FS-CRDS

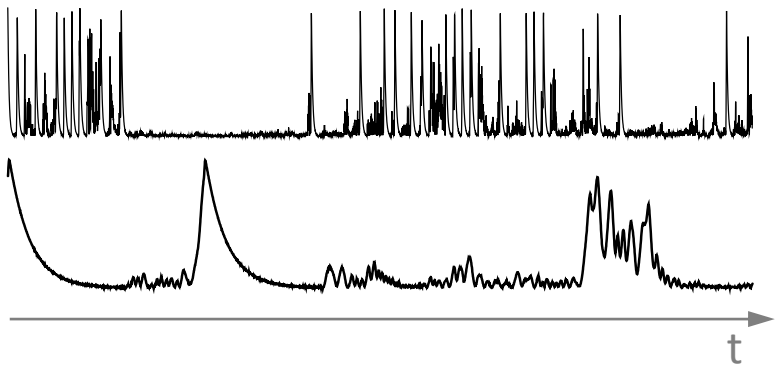

PDH-locked FS-CRDS

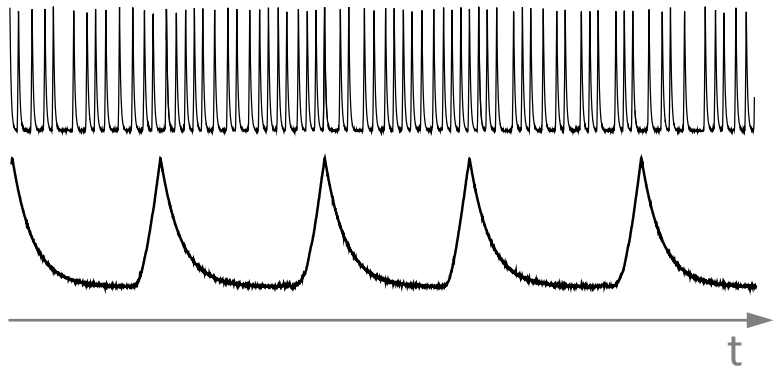

Increase of repetition rate→ faster signal averaging → increase of precision

PDH-locked FS-CRDS

PDH error signal

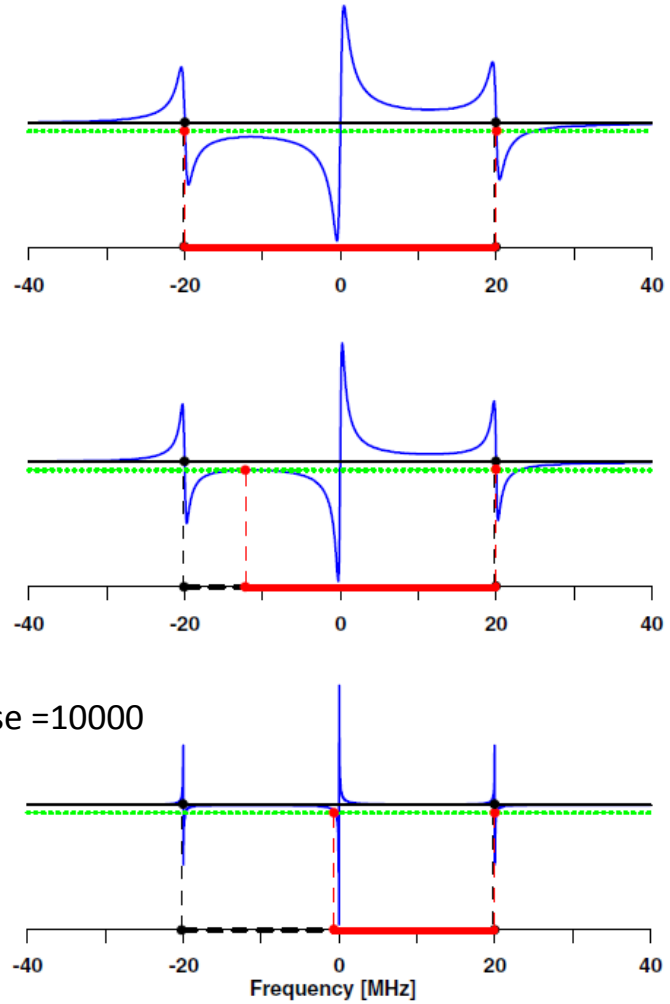

Finesse =10000

interrupted PDH lock

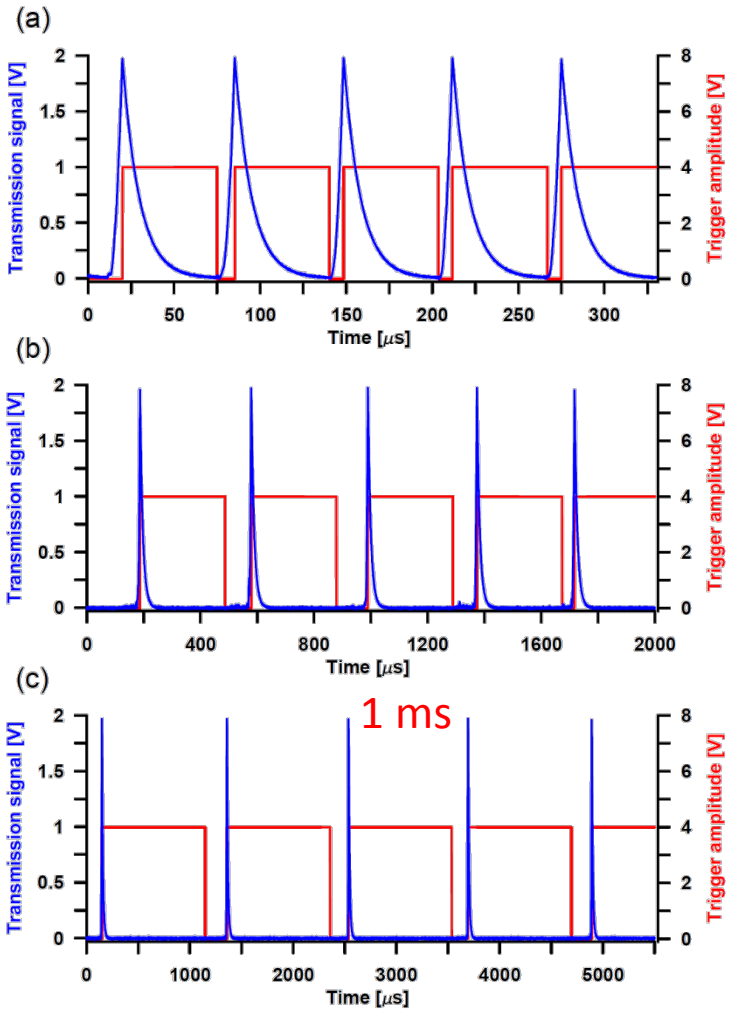

A. Cygan, et al, *Meas. Sci. Technol.* **22**, 115303 (2011).

Saturation CRD spectroscopy – Lamb dips

Non-exponential ring-down signal
due to nonlinear absorption

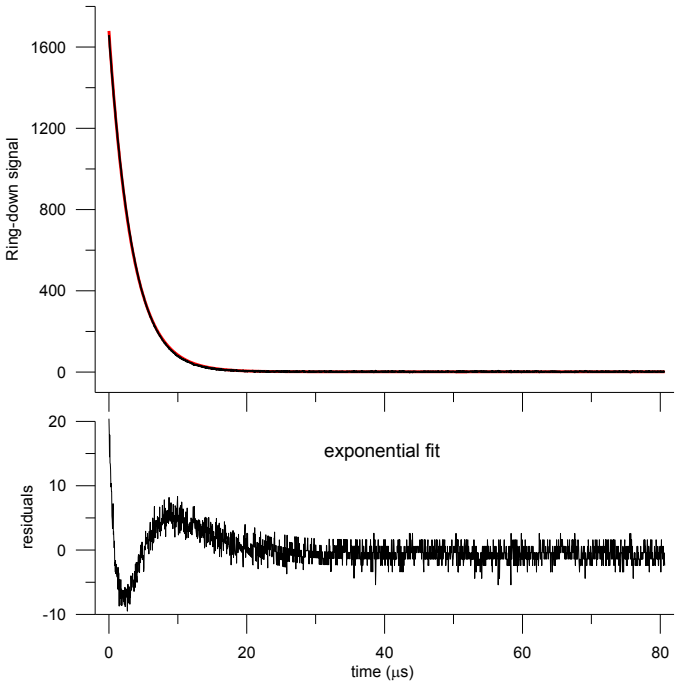

frequency step = 50 kHz
~ 1 MHz-wide dips

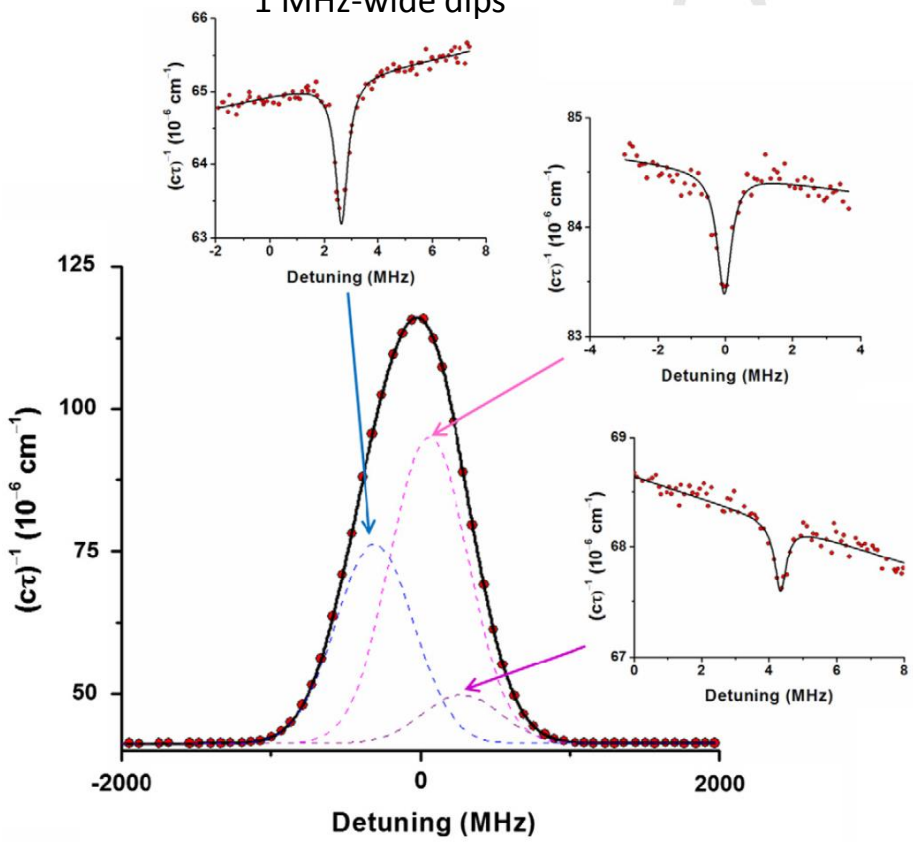

D. Lisak, J. T. Hodges, Appl. Phys. B, **88**, 317-325 (2007)

Some alternative methods based on CEAS

In the vicinity of absorber cavity modes are spectrally broadened due to the absorption and shifted due to light dispersion.

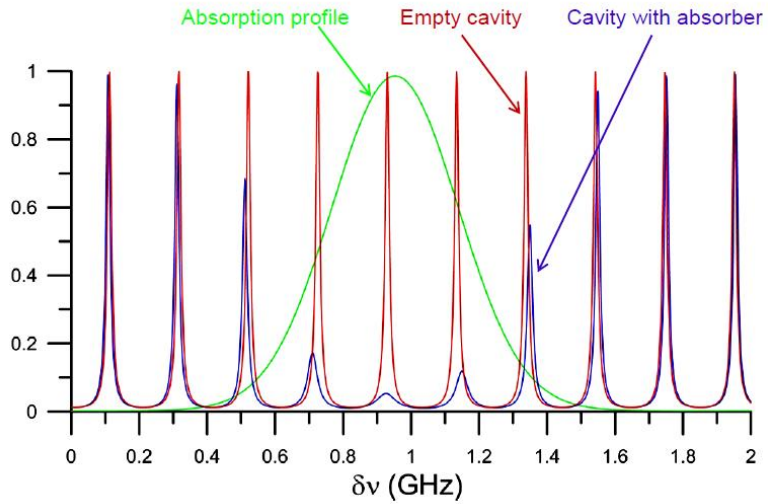

❑ The radiation intensity transmitted through the cavity filled with an absorbing gas is given by the expression:

$$I_T(\nu) = I_0 \frac{(1-R)^2 \mathrm{e}^{-\alpha(\nu)L}}{(1-R\mathrm{e}^{-\alpha(\nu)L})^2} \frac{(1-R\mathrm{e}^{-\alpha(\nu)L})^2}{(1-R\mathrm{e}^{-\alpha(\nu)L})^2 + 4R\mathrm{e}^{-\alpha(\nu)L}\sin^2(\frac{\pi\nu}{\nu_{\mathrm{FSR}}(\nu)})}$$

where $\alpha(\nu)$ – absorption coeffcient, L – cavity length, R – intensity reflectivity of the cavity mirrors, $\nu_{FSR}(\nu)$ – free spectral range of the cavity.

❑ **Measurements in the time domain** → ***Cavity Ring-Down Spectroscopy (CRDS)***

$$\tau(\nu) \approx \frac{L}{c(1-R+\alpha(\nu)L)}$$ ← decay time constant recorded in CRDS

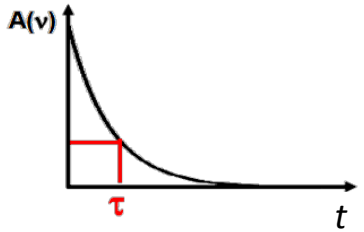

❑ **Measurements in the frequency domain** → ***Cavity Mode-Width Spectroscopy (CMWS)***

$$\delta\nu_m(\nu) \approx \frac{1}{2\pi n \tau(\nu)}$$ ← cavity mode width recorded in CMWS

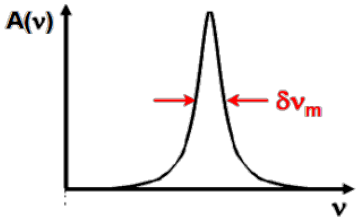

❑ **Measurements in the frequency domain** → ***Cavity Mode-Dispersion Spectroscopy (CMDS)***

$$\nu_{\mathrm{FSR}}(\nu) = \frac{\nu_{\mathrm{FSR_{bg}}}(\nu)}{1 - \frac{\mathrm{Im}(I(\nu))}{4\pi k_0}}$$ ← cavity free spectral range recorded in CMDS

$\nu_{\mathrm{FSR_{bg}}}$ ← FSR far from absorption resonance

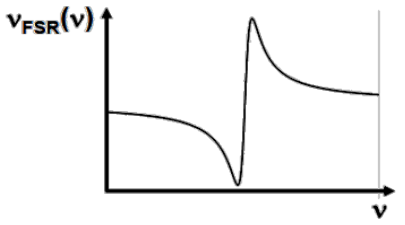

Some alternative methods based on CEAS

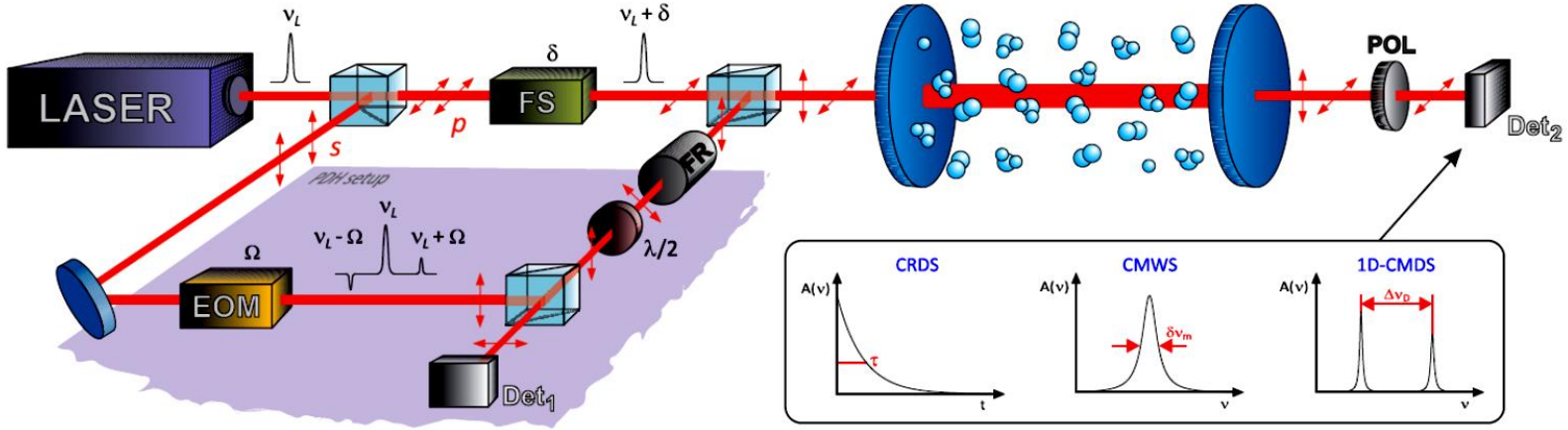

Spectrum of TEM_{00} mode of the optical cavity

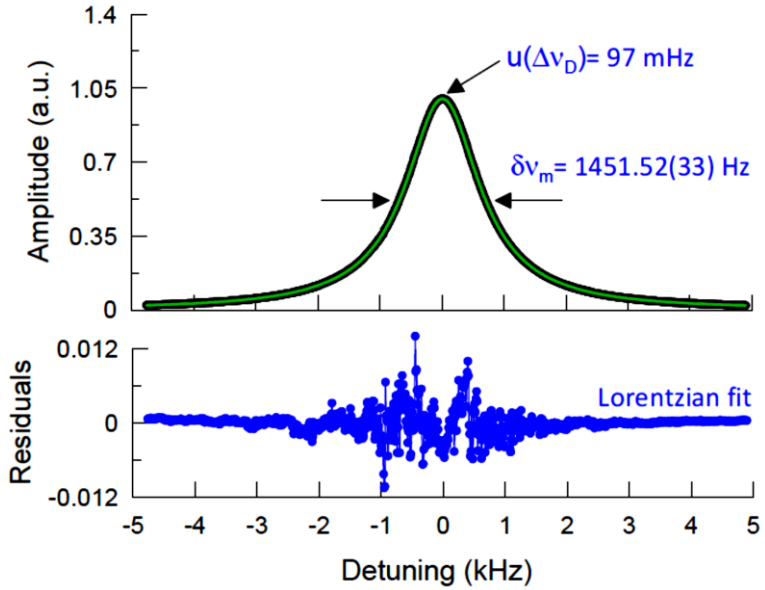

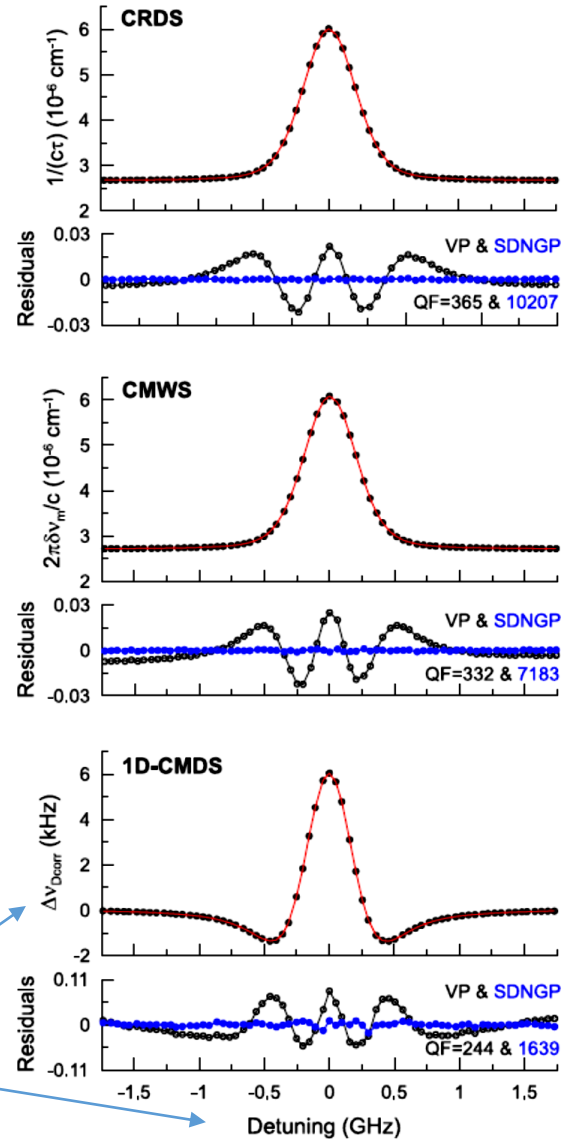

the same frequency on both axes of spectrum

A. Cygan et al., *Opt. Express* **23**, 14472 (2015)

Some alternative methods based on CEAS

Advantages of cavity mode-width spectroscopy:

- linear high-bandwidth detectors not needed
- higher dynamic range than CRDS

  Increase of absorption leads to:
  Shorter decay in CRDS (worse)
  Larger mode width (better)

Advantages of cavity mode dispersion spectroscopy:

- based on frequency measurement only
- insensitive to nonlinearity of detection system
- more sensitive to the line-shape model *

* Wang *et al*. JQSRT **136**, 28 (2014)

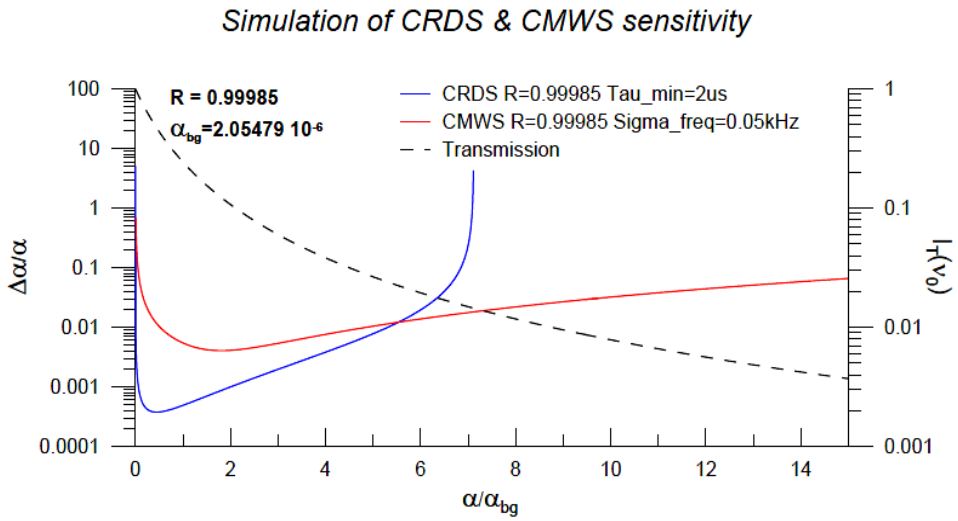

A. Cygan et al., *Opt. Express* **21**, 29744 (2013)

Frequency-agile, rapid scanning (FARS) spectroscopy

Method:

- Use waveguide electro-optic phase-modulator (PM) to generate tunable sidebands
- Drive PM with a rapidly-switchable microwave (MW) source
- Fix carrier and use ring-down cavity to filter out all but one selected side band

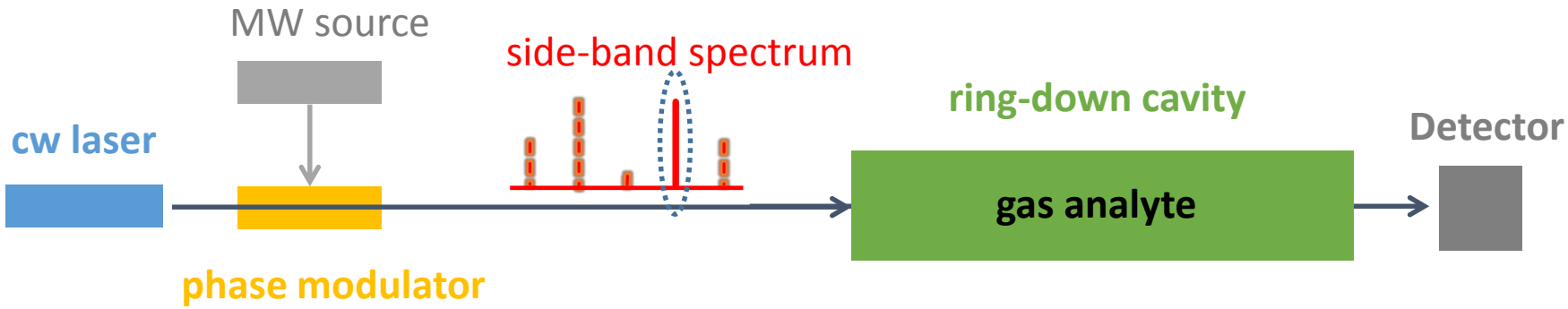

Advantages:

- Overcomes slow mechanical and thermal scanning
- Links optical detuning axis link to RF and microwave standards
- Wide frequency tuning range (> 90 GHz = 3 cm^{-1})

nature photonics
LETTERS
PUBLISHED ONLINE: 28 APRIL 2013 | DOI: 10.1038/NPHOTON.2013.98

Frequency-agile, rapid scanning spectroscopy

G.-W. Truong[1,2], K. O. Douglass[1], S. E. Maxwell[1], R. D. van Zee[1], D. F. Plusquellic[1]*, J. T. Hodges[1] and D. A. Long[1]*

FARS measurement principle

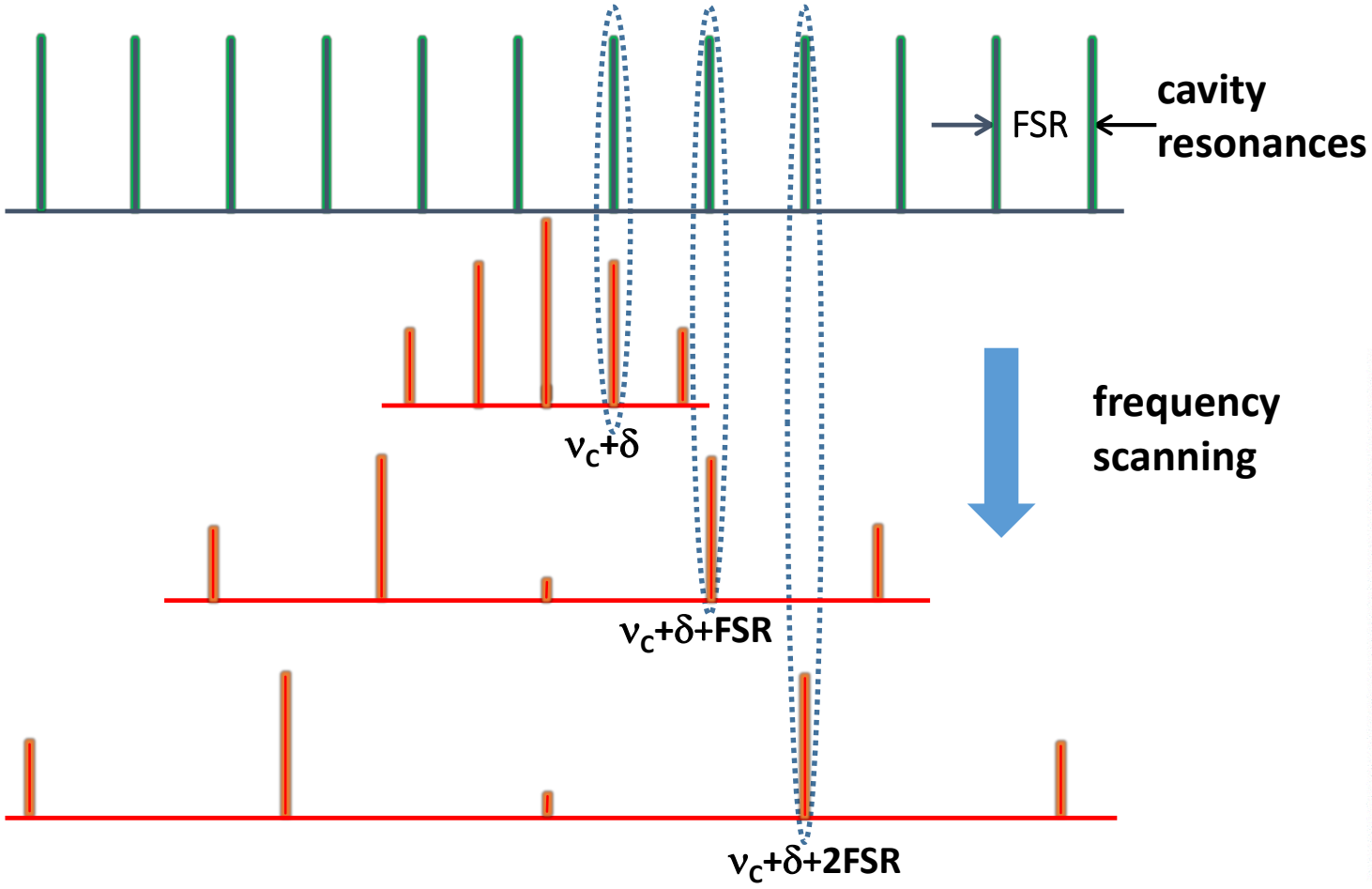

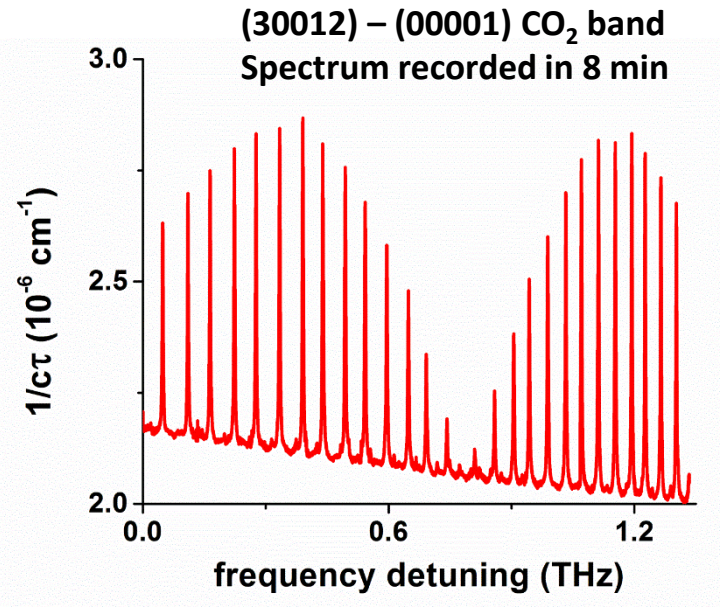

Thank you for your attention

Toruń, Poland